APPROXIMATION of THREE - DIMENSIONAL INHOMOGENJEITIES BY TWO - DIMENSIONAL INHOMOGERELTIES IN MAGNETOTELLUHIC INTERPRETATION

by

Anthony Azunna Onwuegbuche

Submitted in partial fulfilment of the requirements for the degree of master of Science, Applied Geophysics

Department of Physics
Ahmadu Bello University
zaria

July, 19814

ABSTRACT

The approximation of buried simple conductive three - dimensional (3 - D) inhomogeneities by two # dimensional (2 - D) inhomogeneities is investigated numerically using the Rayleigh-FfT modeling technique. The technique is applicable to curved interfaces between regions of different conductivity.

The effects of the increased aspect ratio of the 3 - D models on the apparent resistivities, skew and tipper for the E - parallel and E - perpendicular modes are studied. Also investigated is the behaviour of these quantities when the condition for electrodynamio similitude to exist between two models is satisfied. The results show that 3 - D E - perpendicular mode apparent resistivities and the 2 - D Transverse magnetic (TM) mode, values agree very closely.

The 3 - D E - parallel mode apparent resistivities are sensitive to strike extent and frequency and approach the ? - D Transverse eleotric (TE) mode results as the aspect ratio is increased. It is found that the ratio of the width of the inhomogeneity to the skin depth in the half-space is a very important quantity in predicting the percentage difference between the 2 - D and 3 - D values at a given aspect ratio. Very simple guidelines for the above prediction are given for models having conductivity contrast of 1 : 10 or its powers.

The maximum skew values for the 3 - D models decreased by about 60 percent for a change in aspect ratio from *2* to 4 and ..m remained constant when the aspect ratio is changed from 4 *to* 6.

In general, as the aspect ratio is increased the tipper azimuths around the. middle of the inhomogeneities indicated the long axes of the bodies.

When the condition for similitude to exist between two models is satisfied, it is found that the apparent resistivities are appropriately scaled while the skew values, tipper magnitudes and tipper azimuths are the same for both models.

ACKNOWLEDGEMENT

I am very grateful to Dr. M. A. Daniyan for suggesting and providing the computer programs for this all - exposing project as well as for supervising it. His suggestions and kind supervision throughout the course of this work are highly appreciated.

I wish to thank Professor D.E. Ajakaiye, Head of Department of Physics, Ahmadu Bello University, Zaria, for detailed reading of the draft of this thesis and very useful comments that brought the thesis to this form.

I am greatly indebted to Messers Pat. Kaine, Cletus Ekoja, I. R. Udofia and other staff of the Ahmadu Bello University Computer Centre, Zaria. Probably this work would not have come this far without their help and cooperation during the computations at the ABU computer centre.

A lot of people contributed in one way or another to the success of this work. Among these are Messers R. Anumba, S. I. Babafemi and Joe Eloegbusi all of the Faculty of Science, Ahmadu Bello University, Zaria, Dr. S. K. Park of Chevron Oil Field Research Company, California and Professor G. W. Hohmann of Geology and Geophysics Department, University of Utah. I also express my thanks to Mrs.T. U. A. Ihuoma, who typed this thesis.

Financial aid for this work was provided by the Imo State University in form of a study fellowship.

TABLE OF CONTENTS

	PAGE
ABSTRACT	ii
ACKNOWLEDGEMENT	iv
TABLE OF CONTENTS	v
LIST OF TABLE	vii
LIST OF FIGURES	viii
CHAPTER I	1
INTRODUCTION	1
CHAPTER II	6
GENERAL THEORY OF MAGNETOTELLURICS	6
2.1 Maxwell's Equations	6
2.2 Coordinate System and Model	8
2.3 The Two - dimensional Problem	10
2.4 The Three - dimensional Problem	11
2.5 Solution to Maxwell's equations	12
CHAPTER III	14
THE RAYLEIGH - FFT NUMERICAL TECHNIQUE	14
3.1 Periodicity Assumption	15
3.2 Advantages and Error Sources for the Rayleigh - FFT Technique	18
3.3 Electrodynamic Similitude and the Rayleigh - FFT Technique	19

TABLE OF CONTENTS

		PAGE
CHAPTER IV		24
	MAGNETOTELLURIC RESPONSE FOR CONDUCTIVE INHOMOGENEITIES	24
4.1	Description of the Models	24
4.2	Spatial Variation of Electromagnetic field components	28
4.3	Model Results and Analysis	33
4.4	Applications of the Magnetotelluric Method	49
CHAPTER V		51
	DISCUSSION AND CONCLUSIONS	51
APPENDIX A	SOLUTION TO THE PARTIAL DIFFERENTIAL EQUATIONS	56
APPENDIX B	MAGNETOTELLURIC QUANTITIES	61
REFERENCES.		66

LIST OF TABLES

Table		page
3.1	Model parameters for 'natural' and 'model' systems	22
3.2	Apparent resistivities calculated at centre cross-profile transverse to the long axis of the inhomogeneities 'Natural' and 'model' system	23
4.1	Model parameters for Models 1, 2, 3, 4, 5 and 6.	27
4.2	Apparent resistivities and maximum skew values for Models 1, 2, 3, 4, 5 and 6	34
4.3	Percent changes in apparent resistivities and maximum skew values for different changes in aspect ratio - Models 1, 2, 3, 4, 5 and 6.	35

LIST OF FIGURES

Figure		Page
2.1	Coordinate system and a general subsurface structure.	9
3.1	Truncation number - repetition distance curves for different values of σf	17
4.1	Cross-section of two - and three - dimensional models	25
4.2	Spatial variation of E - parallel mode horizontal field components of a 3 - D body (aspect ratio = 2)	29
4.3	Spatial variation of E - parallel mode horizontal field components of a 3 - D body (aspect ratio = 4)	30
4.4	Spatial variation in TE mode horizontal field components Ex and Hy over a 2 - D body	31
4.5	Plan view of a 3 - D Model	36
4.6	Tipper azimuths and normalized E - parallel mode apparent resistivities - Model 1	37
4.7	Tipper azimuths and normalized E - parallel mode apparent resistivities - Model 2	38
4.8	Tipper azimuths and normalized E - parallel mode apparent resistivities - model 3	39
4.9	Tipper azimuths and normalized E - parallel model apparent resistivities - model 4	40

Figure		page
4.10	Tipper azimuths and normalized E - parallel mode apparent resistivities - model 5	41
4.11	Tipper azimuths and normalized E - parallel mode apparent resistivities - model 6	42
4.12	Field perturbation machanisms.	46

CHAPTER I

INTRODUCTION

Long period electromagnetic (EM) waves originating mostly from complex interactions between the earth's magnetic field and the flow of plasma from the sun and from meteorological activities (Kaufman and Keller, 1981) induce alternating electric currents in the earth. These currents are perturbed by horizontal and vertical anomalies of electrical conductivity in the earth and produce secondary fields which modify the total fields at the earth's surface. The magnetolelluric (MT) method, developed in the 1950's, is an electromagnetic technique, which involves the measurement of the naturally occuring electric and magnetic fields at the surface of the earth as a function of time (Cagniard, 1953). These time domain measurements are analysed to obtain impedances, apparent resistivities and other earth response functions (ERF) which are used in geophysical interpretations to determine the electrical conductivity distributions within the earth. These distributions are then combined with the known relationships between electrical conductivity and geologic materials to infer geologic structures.

Depending on the nature of the target of a survey, one -, two - or three - dimensional modeling is required for quantitative interpretation. In a cartesian coordinate system in which Z is positive downward and for the simplest case of isotropic and homogeneous earth models a one-dimensional (1 - D) model is one in which conductivity depends only on depth. A two-dimensional

(2 - D) model has conductivity varying along one horizontal coordinate and with depth while in a three-dimensional (3 - D) model conductivity varies with both horizontal coordinates and with depth.

In 1 - D environments the earth is assumed to consist of uniform horizontal layers (Cagniard, 1953; Yungul, 1961 and Srivastava, 1967). Responses for 1 - D earth models can be computed as accurately as desired at low computing costs. Among the 2 - D models presented so far are: Vertical contact (d'Erceville and Kunetz, 1962), infinite dike (Rankin, 1962), inhomogeneities of rectangular cross-sections in homogeneous or layered half-spaces (Weidelt, 1975; Ting and Hohmann, 1981 and Park, 1983) and one-dimensionally varying subsurface interface (Mann, 1964 and Jiracek, 1973). The 3 - D interpretational models are in the form of parallelepipeds in a homogeneous or layered half-space of different conductivity (Jones, 1974; Weidelt, 1975; Hohmann, 1975; Reddy et al 1977; Jones and Vozoff, 1978; Ting and Hohmann, 1981; Wannamaker et al , 1982; Newman et al , 1983 and Park, 1983) and two - dimensionally varying subsurface interface separating homogeneous isotropic regions (Jiracek, 1973 and Daniyan, 1983).

In recent years various numerical techniques have been developed to solve the partial differential equations resulting from Maxwell's equations for these 2 - D and 3 - D earth models. They include: finite difference (Neves, 1957), transmission surface analogy (Swift, 1967), finite element (Silvester and Haslam, 1972 and Reddy et al , 1977), integral equations (Hohmann, 1975; Weidelt, 1975; Meyer 1976; Ting and Hohmann, 1981 and Wannamaker et al , 1982), Rayleigh- FFT (Jiracek, 1973 and Daniyan, 1983) and thin

sheet analysis (Park, 1983).

All the above techniques have the merit that for 2 - D models they are relatively easy to implement in the computer and do not require large computer memory allocation and computation time. For 3 - D models one of the main problems is that they require large memory allocation; another is that excessive computer times are needed. For example it took about 30 minutes on a CDC 6600 to obtain solutions, using Daniyan's (1983) 3 - D Rayleigh - FFT modeling algorithm for one source polarization, for a body with a maximum interface slope of 18 degrees. It took 156 minutes on a Univac 1108 to obtain the electric field components for Reddy et al , (1977) 3 - D finite element modeling technique. The integral equation technique by Wannamaker et. al (1982) took about 20 hours on a Prime 400 for an inhomogeneity buried in a layered half-space. In the second and third examples above symmetry conditions were applied to reduce computational effort.

Also in order to have a better understanding of the subsurface structure through 3 - D MT modeling, data from the field should be collected in a grid pattern (Daniyan, 1983). This procedure is very expensive; for example, the average survey cost per site for petroleum prospecting in the United States of America in 1981 was about 2,700 dollars (Senti, 1982).

The high computing costs and the very expensive procedure of obtaining data from the field in a grid pattern have raised questions about the economical feasibility of 3 - D MT modeling

thereby making 3 - D surveys and interpretations far less attractive than 2 - D ones. These facts led some workers, notably Weidelt (1975), Ting and Hohmann (1981), Daniyan (1983) and Park (1983) to investigate the circumstances under which a 3 - D body may be approximated by a 2 - D body. Weidelt (1975) investigated the transition from a three - to a two - dimension of a conductive inhomogeneity in the form of a parallelepiped in a half-space. He computed the transverse electric (TE) mode EM field components at a single frequency for different length to width ratios (aspect ratios) and concluded that a 2 - D description is adequate if the aspect ratio of the body is greater than 3. Ting and Hohmann (1981) asked the question: "How long must an elongated prism be before its response will resemble that of a 2 - D structure?" They noticed that the answer to the above question, depends not only on the mode of polarization (E - parallel or E - perpendicular) but is also heavily influenced by the frequency of the incident waves. Daniyan (1983) observed that for a 3 - D body to be approximated by a 2 - D body the corners have to be reasonably far apart; how far apart they will be depends on the skin depths in the half-space and inhomogeneity. Park (1983) did a work similar to Weidelt's (1975) and arrived at about the same conclusions as Weidelt (1975) by looking at the apparent resistivities instead of the field components.

In this work we shall carry out a systematic study on the approximations of 3 - D bodies by 2 - D ones, keeping in mind the observations made by Weidelt (1975), Daniyan (1983) and

Park (1983) as well as the question raised by Ting and Hohmann (1981). The aim is to find some guidelines so that 2 - D survey and modeling could be carried out in place of 3 - D ones without much loss of the desired information.

Earth's surface electric and magnetic fields will be computed for some models using Daniyan's (1983) 3 - D and 2 - D computer programs based on the Rayleigh - FFT technique. The technique is applicable to curved interfaces between regions of different conductivity.

The behaviour of some MT quantities such as apparent resistivities, skew, tipper magnitude and tipper azimuth as the aspect ratio of a buried simple conductive 3 - D inhomogeneity is increased will be investigated. Also to be investigated is the behaviour of these quantities when electrodynamic similitude is invoked.

CHAPTER II

GENERAL THEORY OF MAGNETOTELLURICS

The natural electromagnetic fields measured at the surface of the earth at any given location contain information about the source of the fields as well as the structure and conductivity distribution of the subsurface. These field are total fields comprising the field of alternating currents induced in the earth and the extraneous field inducing the currents. These fields obey Maxwell's equations and the forward problem involves the solution of these equations for a given model and boundary conditions.

2.1 Maxwell's Equations.

Maxwell's equations govern large scale electromagnetic phenomena. These equations are

$$\text{Curl } \bar{E} = -\frac{\partial \bar{B}}{\partial t} \qquad (1)$$

$$\text{Curl } \bar{H} = \bar{J} + \frac{\partial \bar{D}}{\partial t} \qquad (2)$$

The consititutive relations for linear, isotropic, and homogeneous media are

$$\begin{aligned} \bar{B} &= \mu \bar{H} \\ \bar{D} &= \varepsilon \bar{E} \\ \bar{J} &= \sigma \bar{E} \end{aligned} \qquad (3)$$

where

$\bar{E}$ is the electric field intensity in volts/metre.

$\bar{H}$ is the magnetic field intensity in ampere-turns/metre

$\bar{B}$ is the magnetic induction in webers/metre.^{2}

$\bar{D}$ is the electric displacement in coulombs/metre.^{2}

t is time

σ is the electrical conductivity in mhos/metre.

μ is the magnetic permeability of free space.

ε is the permittivity of free space.

In MT work, plane electromagnetic waves with exp(iwt) time dependence are usually assumed to be normally incident on an air-earth interface (a flat air-earth interface is assumed in this study). Also μ and ε are assigned their free space values.

Thus equations (1) and (2) can be written as

$$\text{Curl } \bar{E} = -iw\mu\bar{H} = -\hat{Z}\bar{H} \qquad (1a)$$

$$\text{Curl } \bar{H} = (\sigma + iw\varepsilon)\bar{E} = \hat{Y}\bar{E} \qquad (2a)$$

where $i = \sqrt{-1}$, $\hat{Y} = \sigma + iw\varepsilon$ and $\hat{Z} = iw\mu$

w is the radian frequency in seconds $^{-1}$.

By taking the curl of equation (1a) and substituting Curl $\bar{H}$ from equation (2a) and similarly taking the curl of equation (2a) and substituting curl $\bar{E}$ from equation (1a), two identical equations are obtained:

$$\nabla^2\bar{E} - \nabla(\nabla \cdot \bar{E}) = \hat{Z}\hat{Y}\bar{E} \qquad (1b)$$

$$\nabla^2\bar{H} - \nabla(\nabla \cdot \bar{H}) = \hat{Z}\hat{Y}\bar{H} \qquad (2b)$$

Let $\bar{R}$ represent either $\bar{E}$ or $\bar{H}$ then

$$\nabla^2\bar{R} - \nabla(\nabla \cdot \bar{R}) = \hat{Z}\hat{Y}\bar{R} \qquad (4)$$

2.2 Coordinate System and Model.

The cartesian coordinate system (Figure 2.1) is used for all the models in this work. The origin of the system O is at the ground surface. The Z axis is positive downward and the X and Y axes are in two perpendicular horizontal directions. Figure 2.1 shows a cross - section of the general subsurface structure used. The air-earth interface is flat; the first subsurface interface varies in one direction (2 - D case) or in two directions (3 - D case) while with second subsurface interface is planar. The air layer has a zero conductivity, σ_0 , and the other layers have conductivities σ_1 , σ_2 and σ_3 respectively. Subscripts are indices of the different regions as follows:

Index of region	region
0	$Z < 0$
1	$A + F(Y) > Z > 0$ (2-D case) $A + F(X,Y) > Z > 0$ (3-D case)
2	$D > Z > A + F(Y)$ (2-D case) $D > Z > A + F(X,Y)$ (3-D case)
3	$Z > D$

A and D represent depth,

To model a conductive inhomogeneity in a homogeneous half-space, D is made equal to A while the value of σ_3 equals that of σ_1 and σ_2 is greater than σ_1 .

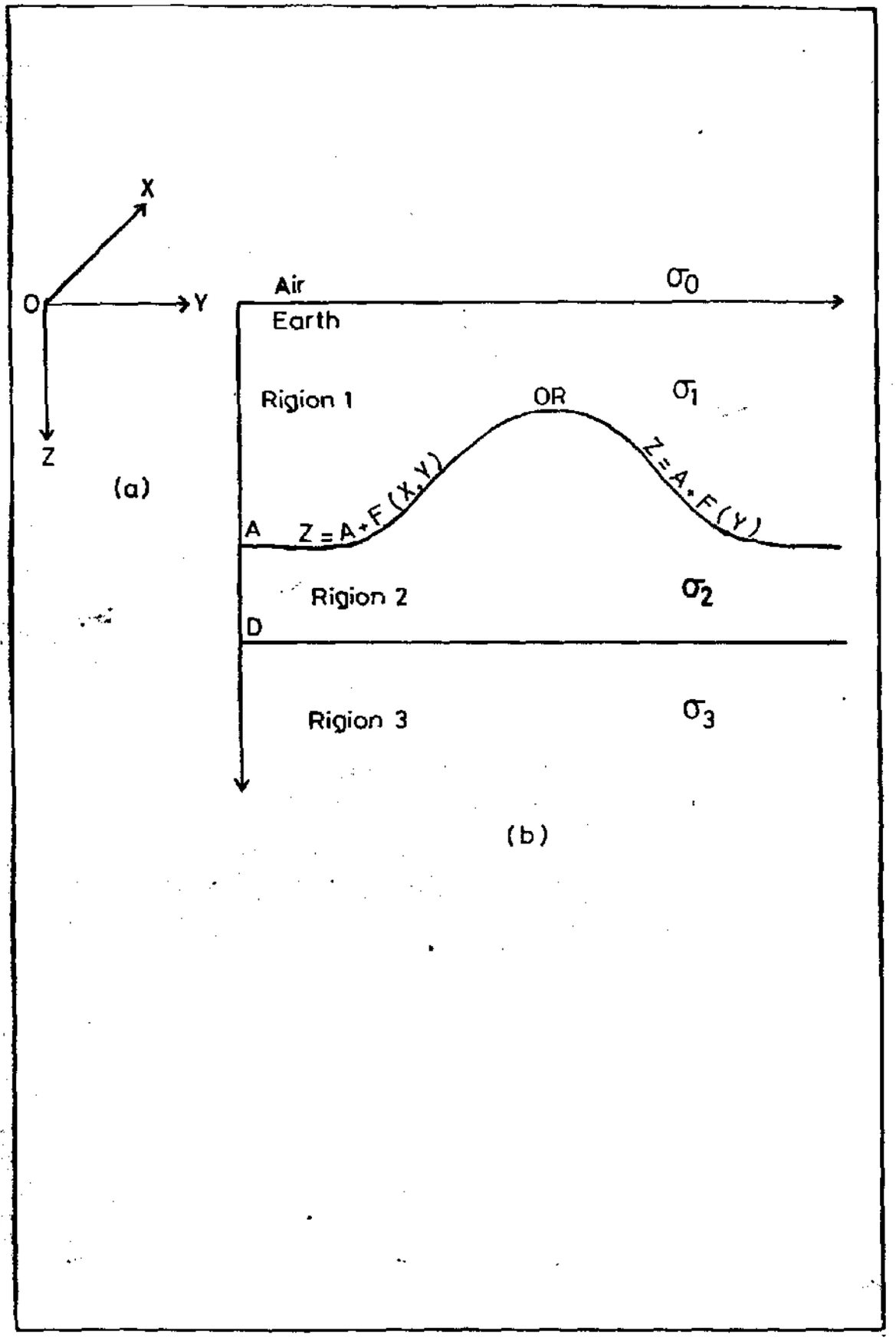


FIG. 2-1 (a) Coordinate system and (b) a general subsurface structure.

2.3 The Two - dimensional Problem.

In a two - dimensional structure the scalar conductivity varies in one horizontal direction and with depth. The other horizontal direction is the strike of the structure (the X-direction in Figure 2 . 1).

Maxwell's equations (1a. and 2a.) decouple into two independent sets of equations when a 2 - D structure is excited by a plane wave source and the X and Y coordinate axes coincide with the principal directions defined parallel and perpendicular to strike as in Figure 2.1. One set is for the case where the incident electric field is parallel to the strike and is referred to as the transverse electric mode or TE mode while the other set is for the situation when the incident magnetic field is parallel to the strike and is called the transverse magnetic mode or TM mode. Here, TE mode field components are Ex, Hy, and Hz while the TM mode field components are Hx, Ey and Ez. Mode identification is determined by the single component of electric or magnetic field for each mode which is parallel to the strike of the anomaly.

Maxwell's equations corresponding to these two modes are:

for TE mode (using equations (1a) and (2a))

$$\frac{\partial Hz}{\partial y} - \frac{\partial Hy}{\partial z} = \hat{Y}\, Ex \qquad (5a)$$

$$\frac{\partial Ex}{\partial z} = - \hat{Z}\, \bar{H}y \qquad (5b)$$

$$\frac{Ex}{\partial y} = \hat{Z}\, Hz \qquad (5c)$$

and for TM mode

$$\frac{\partial Ez}{\partial y} - \frac{\partial Ey}{\partial z} = - \hat{Z}\, Hx \qquad (6a)$$

$$\frac{\partial Hx}{\partial z} = \hat{Y}\, Ey \qquad (6b)$$

$$-\frac{\partial Hx}{\partial y} = \hat{Y}\, Ez \qquad (6c)$$

Solutions to the above system of equations, evaluated at the surface of the earth model, yield the magnetotelluric field components at the earth's surface.

2.4 The Three - dimensional Problem.

The conductivity structure is more complicated in three - dimensional models and the scalar conductivity, σ, varies in two perpendicular horizontal directions and with depth. There is usually no defined strike and Maxwell's equations for 3 - D structure excited by a plane wave source do not generally decouple. All the components of the electromagnetic field are always present when the incident electric field is polarized in a particular direction. When the incident electric field is parallel to the long axis of the body the mode of polarization is termed E - parallel and when it is perpendicular to the long axis it is termed E - perpendicular mode of polarization (cf. TE and TM modes of polarization respectively)

The vector equation, (4), may be written as three scalar equations in cartesian coordinates:

$$\frac{\partial^2 Rx}{\partial y^2} + \frac{\partial^2 Rx}{\partial z^2} - \frac{\partial}{\partial x}\left(\frac{\partial Ry}{\partial y} + \frac{\partial Rz}{\partial z}\right) = \hat{Z}\,\hat{Y}\, Rx \qquad (7a)$$

$$\frac{\partial^2 R_y}{\partial x^2} + \frac{\partial^2 R_y}{\partial z^2} - \frac{\partial}{\partial y}\left(\frac{\partial R_x}{\partial x} + \frac{\partial R_z}{\partial z}\right) = \hat{Z}\,\hat{Y}\,R_y \quad (7b)$$

$$\frac{\partial^2 R_z}{\partial x^2} + \frac{\partial^2 R_z}{\partial y^2} - \frac{\partial}{\partial z}\left(\frac{\partial R_x}{\partial x} + \frac{\partial R_y}{\partial y}\right) = \hat{Z}\,\hat{Y}\,R_z \quad (7c)$$

Again the solutions of the above simultaneous equations, evaluated at the earth's surface, are the magnetotelluric field components for 3 - D anomalies of electrical conductivity.

2.5 Solutions to Maxwell's Equations

The partial differential equations resulting from Maxwell's equations are reduced to ordinary differential equations using the Fourier integral transform technique (Appendix A) and solved in the usual manner. The results are:

for 2 - D models

$$R_{lx}(y,z) = \frac{1}{2\pi}\int_{-\infty}^{\infty}\left[A_l(\eta)\exp(\alpha_l z) + B_l(\eta)\exp(-\alpha_l z)\right]\exp(i\eta y)\,d\eta \quad (8a)$$

and for 3-D models

$$R_{lx}(x,y,z) = \frac{1}{4\pi^2}\int_{-\infty}^{\infty}\int_{-\infty}^{\infty}\left[C_l(\xi,\eta)\exp(\alpha_l' z) + D_l(\xi,\eta)\exp(-\alpha_l' z)\right]\times \exp(i\xi x + i\eta y)\,d\xi\,d\eta \quad (8b)$$

where R_{lx} represents either the magnetic or electric field component along the X-direction in the region l which can be calculated for any coordinate position (y, z) or (x, y, z).

α_l and α_l' are the propagation constants; A_l, B_l, C_l and D_l are the spectral amplitudes and ξ, η are the wave-numbers in the horizontal coordinates directions.

In order to evaluate the field components, the unknown quantities in the above expressions which are the spectral coefficients A_l, B_l etc. must be determined. To find them the usual electromagnetic boundary conditions are enforced. These conditions for a boundary between two media of finite conductivity are:

$$\hat{\eta} \times (\bar{H}_1 - \bar{H}_2) = 0$$

$$\hat{\eta} \times (\bar{E}_1 - \bar{E}_2) = 0;$$

$\bar{H}1$ and $\bar{H}2$ are the magnetic fields in adjacent regions, 1 and 2 and $\bar{E}1$ and $\bar{E}2$ are the corresponding electric fields. $\hat{\eta}$ is the unit vector normal to the interface. The application of the above boundary conditions at the interfaces results in coupled integral equations (Aki and Larner, 1970) which are solved numerically using the Rayleigh - FFT technique to obtain the spectral coefficients. Once the Rlx's are evaluated the complete electromagnetric field components can be found by using either Ampere's or Faraday's law as the case may be.

CHAPTER III

THE RAYLEIGH - FFT NUMERICAL TECHNIQUE

The numerical technique used in solving the coupled integral equations mentioned earlier is the Rayleigh - FFT technique. This technique is applicable to curved interfaces between regions of different conductivity.

The Rayleigh - FFT technique was developed by Aki and Larner (1970) where they used it to evaluate the seismic response of irregular interfaces to plane seismic waves. Bard and Bouchon (1980 a, b) used the technique to study the seismic response of sediment filled valleys . Jiracek (1973) employed it in MT work and computed the MT response for one dimensionally varying interfaces at high frequencies. Daniyan (1983) extended Jiracek's work to computing MT response for two-dimensionally varying interfaces.

In MT studies the target of the techique is to evaluate the electromagnetic response of bodies with non-planar interfaces to a plane-incident electromagnetic wave. The technique depends in part on the Rayleigh representation of the scattered wave field produced by a plane wave incident on a corrugated periodic surface. The scattered electromagnetic field is described as a linear combination of plane waves having discrete horizontal wave numbers (equations (8a) and (8b)). The application of the electromagnetic continuity conditions at the interfaces leads to a system of equations (simultaneous integral equations). These integral equations are solved after being Fourier transformed in

space and truncated. The technique takes advantage of the Fast Fourier Transform to compute the spectral coefficients in the wave number domain.

3.1 Periodicity Assumption.

The Rayleigh - FFT technique assumes that the zone containing the non-planar interface is periodic with periodicity length L along the coordinate axes. If $Z = f(y)$ defines the non-planar interface for a 2 - D model, then

$$f(y) = f(y + mLy), \quad m = 0, \pm 1, \pm 2 \ldots\ldots\ldots$$

Ly is the periodicity length along the y - azis (also called the repetition distance) and

$$\exp(i\eta y) = \exp\left[i\eta (y + Ly)\right]$$

hence

$$\eta = \frac{2\pi m}{Ly} \qquad m = 0, \pm 1, \pm 2 \ldots\ldots\ldots$$

Thus the scattered plane waves have a discrete rather than a continous spectrum of wave numbers. The scattered directions, θy's, of the scattered waves (along the y - direction) are given by

$$K_1 \sin \theta y\,(m) = \frac{2\pi m}{Ly} \qquad (9)$$

where $K_1 = \sqrt{\mu\omega\sigma_1}$, 1 is the index for a given region and m is called the truncation number.

In all the 3 - D models used in this work the repetition distance along the x and y directions, Lx and Ly respectively, are equal. In this case equation (9) yields the same results for 2 - D and 3 - D problems.

The effect of the periodicity assumption is to convert infinite integrals in the coupled integral equations to infinite summations. The infinite summations can be truncated by a suitable choice of m to yield a system of linear equations which are solved in the wave number domain to obtain the spectral coefficients of the electromagnetic field components.

Equation (9) is a very important parametric equation in the Rayleigh - FFT modeling technique containing parameters of the source of EM fields, survey targets and the numerical technique. From it the total number of scattering orders (corresponding to $2m + 1$ wave numbers) required to obtain solutions, for a particular problem, can be obtained. To obtained accurate solutions, the scattering order has to be such that all the angles of scattering up to 90 degrees and usually a few more are included in the solution (Daniyan, 1983). The equation is presented in a graphical form, for some parameters in Figure 3.1. The values of the product of the conductivity, σ, of the anomaly and the frequency f of the incident plane waves, i.e. σf, are also shown in the diagram. From the graphs shown in Figure 3 . 1 the following can easily be observed (for constant permeability, μ):

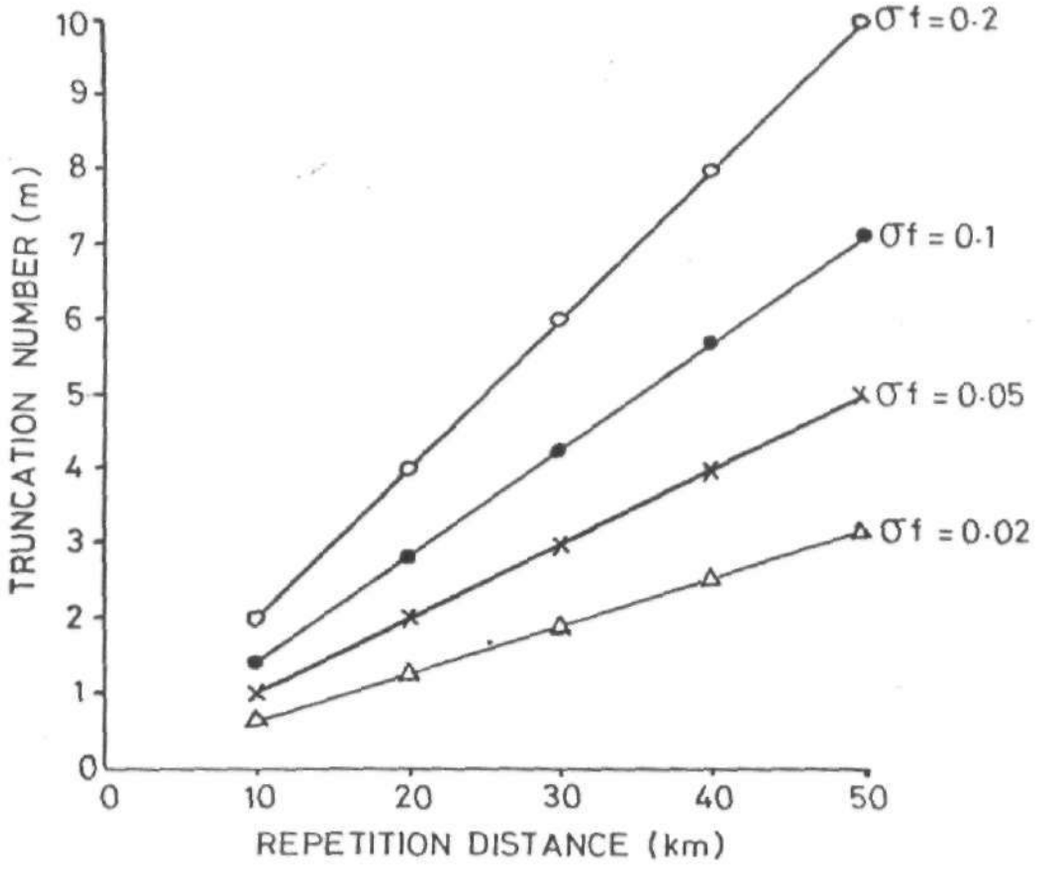


FIG. 3.1 Truncation number – repetition distance curves for different values of σf.

(a) For a given truncation number the repetition distance increases as σf descreases.

(b) As σf increases the truncation number for a given repetition distance increases.

(c) The slope of the truncation number - repetition distance curve increases as σf increases.

Thus for any particular problem, the optimum modeling parameters can easily be deduced from the graphical presentation equation (9).

3.2 Advantages and Error Sources for the Rayleigh - FFT Technique.

The Rayleigh - FFT technique has a very simple mathematical formulation. It is an efficient technique for modeling structures with gently varying slopes and can model both simple and complex geologies. Also both high and low resistivity contrasts as well as very shallow and deeply buried inhomogeneities in a homogeneous or layered half-space could be modelled. Another advangate of the technique is that after a set of field components have been obtained, no numerical differentiation is needed to obtain the other set. Numerical differentiation results in crude approximations at boundaries. The Rayleigh - FFT algorithm is very fast in the computer when compared with the other numerical algorithms.

However, the Rayleigh - FFT technique contains three sources of errors. The first and the most important arises from the approximate description of the wave field within the range of

variations of the interface depth (by this technique). The resulting error named 'Rayleigh ansatz' error grows rapidly for large mean interface slopes. Jiracek (1973) suggests that for a perfect electrical conductor the slope should be less than 0.6 to avoid intolerable errors.

The second error comes from the periodicity assumption in the interface shape. Adjacent zones may introduce parasitic effects in the solutions. This problem is minimized by choosing adequate computational parameters such that the repetition distances are large enough for the edge of the inhomogeneity to be at least one skin depth from the outside boundary of the zone under consideration (Daniyan, 1983).

The last error is the trancation (approximation) to a finite number of plane waves. This truncation determines the number of scattering order $(2m+1)$ to be included in a solution. The larger the number of scattering order the more reliable the results become.

The above errors can be controlled to a large extent by selecting suitable modeling Parameters. However the best way of testing the reliability of the solutions is by checking the extent to which the boundary conditions conditions across the non-planar interface are satisfied.

3.3 Electrodynamic similitude and the Rayleigh - FFT Technique.

The MT response of a model of a fixed resistivity contrast as a function of frequency or resistivity can be predicted from

the response of another resistivity model at a single frequency by invoking electrodynamic similitude (Stratton, 1941). When displacement currents are ignored the condition of similitude requires that the characteristic number.

$$C = w\mu\sigma l^2$$

be invariant at each field point to scale changes in the parameters (Cagniard, 1953; d'Erceville and Kunetz, 1962). Here, l represents a length scaling applied to all linear dimensions.

When μ and l are the same for two models, the characteristic number can be represented by σf and the invariance of σf then becomes the condition for similitude to exist between the models. In relation to the Rayliegh - FFT technique this means that the same truncation number - repetition distance graph is obtained for all combinations of resistivity and frequency which leave σf invariant at each field point.

The behaviour of some MT quantities such as apparent resistivities, skew, tipper magnitude and tipper azimuth when σf is invariant at each field point was investigated. These quantities are defined in appendix B.

Two models of identical geometry and same linear dimensions were considered. The first model whose MT response is assumed known is here called the 'natural' system while the other whose MT response is to be predicted from the natural system is called the 'model' system.

The model parameters for the two systems are given in table 3.1. They are also evident in Figure 3.1. To preserve the invariance of f found for the natural system, the frequency and resistivities in the model system were made equal to half of those in the natural system.

It is found that the apparent resistivity values of the natural system are twice those of the model system while the skew, tipper magnitudes and tipper azimuths have the same values in both systems (see table 3.2 for apparent resistivity values for the two models calculated at the centre cross - profile transverse to the long axis of the inhomogeneities; only half of the profile is tabulated because of symmetry).

Generally the results for specific frequencies, resistivities and length scaling apply for any combination of frequency, resistivity and length scaling which preserve invariance of C at each field point.

Electrodynamic similitude was used to reduce computational effort in this work. The details are shown in the next chapter.

TABLE 3.1. Model Parameters for the natural and model Systems

System	Conductivity σ (mhos. M^{-1}) half-space	inhomogeneity	Frequency f (hz)	σ_f	Truncation number	Repetition distance (KM)
Natural	0.005	0.05	1.0	0.05	4	40
Model	0. 01	0.1	0.5	0.05	4	40

Table 3.2. Apparent resistivities calculated at the Centre Cross - profile transverse to the long axis of the inhomogeneities - 'natural' and 'Model' systems.

Distance from Centre of inhomogeneity (KM)	E-Parallel mode apparent resistivity (Ω.M)		E-Perpendicular mode apparent resistivity (Ω.M)	
	Natural system	Model system	Natural System	Model System
10.00	185.5	92.7	164.1	82.1
7.50	215.0	107.5	260.1	130.0
5.00	192.7	96.4	283.2	141.6
2.50	109.6	54.8	132.8	66.4
0.00	73.4	36.7	61.5	30.7

CHAPTER IV

MAGNETOTELLURIC RESPONSE FOR CONDUCTIVE INHOMOGENEITIES

The forward problem in magnetotellurics involves the selection of a realistic earth model and computing its MT response which are used in the interpretation of geophysical field data. In this chapter the 2 - D and 3 - D models studied are described and the resultant fields, apparent resistivities, skew and tipper azimuths are presented and analysed. Also included are the applications of the MT method in geophysical exploration.

4.1 Description of the Models

The models used here consist of an inhomogeneity in an otherwise homogeneous half-space. These are generated from the general model (Figure 2.1) as described earlier; a section view is shown in Figure 4.1. For 2 - D problems the models are infinite in one direction (x - direction here) while for 3 - D problems they are of limited extent in all directions but still elongated in the x - direction. The non-planar subsurface interface in Figure 4.1 is described as follows:

for 2 - D model

$$F(y) = H \qquad \text{for} \quad |y| < d1y$$

$$F(y) = \frac{H}{2}\left[1 + \frac{\cos \pi (y - d1y)}{d2y}\right] \qquad \text{for } d1y < |y| < d1y + d2y$$

$$F(y) = 0 \qquad \text{for } |y| > d1y + d2y$$

and for 3 - D model

$$F(x,y) = H \qquad \text{for } |x| < d1x \text{ and } |y| < d1y$$

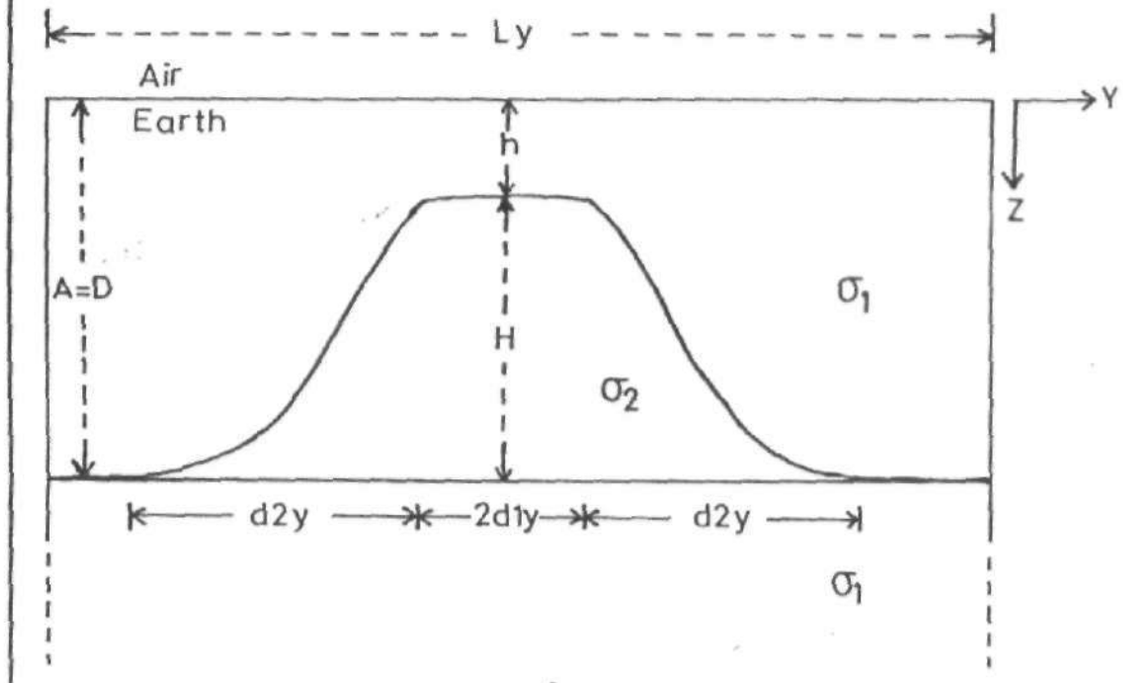


FIG. 4.1 Cross-section of two- and three-dimensional models.

$$F(x,y) = \frac{H}{4}\left[1 + \text{Cos}\frac{\pi(x-d1x)}{d2x}\right]\left[1 + \frac{\text{Cos}\,\pi\,(y-d1y)}{d2y}\right]$$

for $d1x < |x| < d1x + d2x$

and $d1y < |y| < d1y + d2y$

$F(x,y) = 0$ for $|x| > d1x + d2x$ and $|y| > d1y + d2y$

H is the height of the inhomogeneity while h is its depth of burial. A is the mean depth to the first subsurface interface and is equal to the mean depth to the second subsurface interface D. For 3 - D models the lengths of the inhomogeneity at the base in the x and y directions are $2(d1x + d2x)$ and $2(d1y + 2d2y)$ respectively.

The parameters of all the models used are given in table 4.1. The total number of scattering order needed to obtain adequate solutions is equal to 9 in each case. Also $d2x = d2y = d2$ and the repetition distances in the x and y directions are equal. The depth of burial for all the models is fixed at 10 metres. The resistivity contrasts and the cross-sections transverse to the long axis of the 3-D models are the same as those of their corresponding 2 - D models. All the models are symmetric.

TABLE 4.1 Model Parameters for Models 1, 2, 3, 4, 5, and

Model	Resistivity (Ω.M)		Frequency (Hz)	Skin depth (KM)		H	d1y (M)	2(d1y+d2)	Repetition distance (KM)
	Half-space	inhomogeneity		half-space δ_1	inhomogeneity δ_2				
1	50	5	0.556	4.772	1.509	300 M or $0.199\delta_2$	200	2KM or $0.419\delta_1$	20
2	50	5	1.00	3.557	1.125	300 M or $0.267\delta_2$	200	2KM or $0.562\delta_1$	20
3	50	5	1.50	2.904	0.918	300 M or $0.327\delta_2$	200	2KM or $0.689\delta_1$	20
4	100	10	0.50	7.113	2.249	400 M or $0.178\delta_2$	250	3 KM or $0.422\delta_1$	30
5	90	9	1.00	4.772	1.509	300 M or $0.199\delta_2$	200	2 KM or $0.419\delta_1$	20
6	90	5	1.00	4.772	1.125	300 M or $0.267\delta_2$	200	2 KM or $0.419\delta_1$	20

4.2 Spatial Variation of Electromagnetic Field Components.

Large scale electromagnetic induction is responsible for regional electric fields and currents. These fields and curents are perturbed by lateral and vertical conductivity discontinuities in a homogeneous half-space (or any other medium) and consequently the fields on and off the anomalies are distorted. The conductivity anomalies are either two - or three - dimensional. In two - dimensional structures currents are confined to flow in vertical planes. However, in the three - dimensional case currents are not confined to flow in planes but may be deflected laterally by regions of different conductivity. These differences in current flow patterns result in different field behaviour over 2 - D and 3 - D structures.

The spatial variation in the horizontal field components for 2 - D TE and 3 - D E - parallel modes for different aspect ratios anf frequencies are here presented below. Familiarity with the spatial variation in the field components will be an advantage in the understanding of the behaviour of the theoretically computed apparent resistivities presented later.

Models 1, 2 and 3 (table 4.1) were used in studying the spatial variation of the field components. Horizontal field components for each model were caclulated for three length to width ratios (aspect rations) namely 2, 4 and ∞ . The amplitudes of the field components are plotted on a linear scale in Figures 4.2, 4.3 and 4.4 after normalization by the distant field.

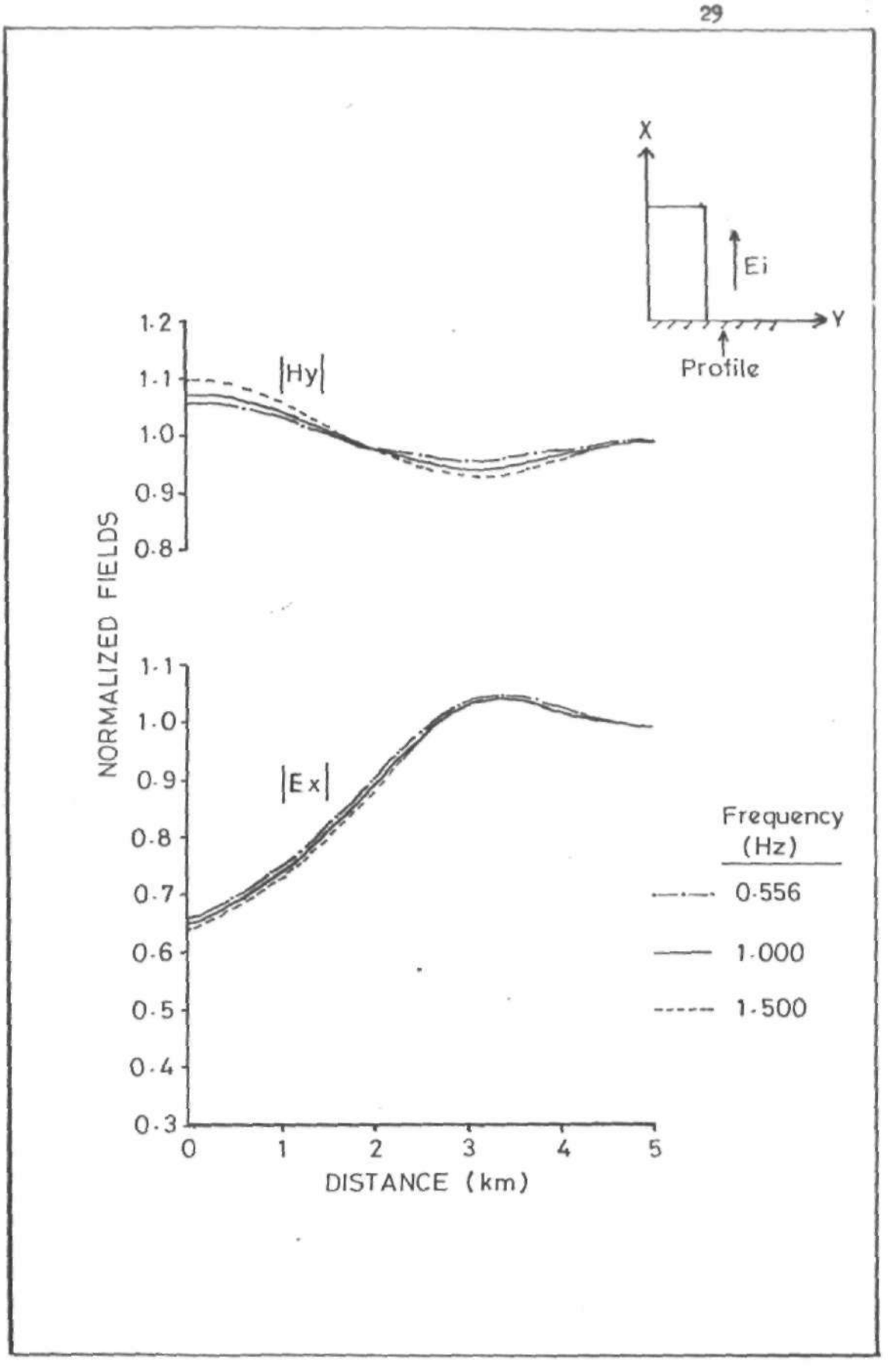


FIG. 4.2 Spatial variation of E-parallel mode horizontal field components of a 3-D body (aspect ratio = 2) Ei is the incident electric field.

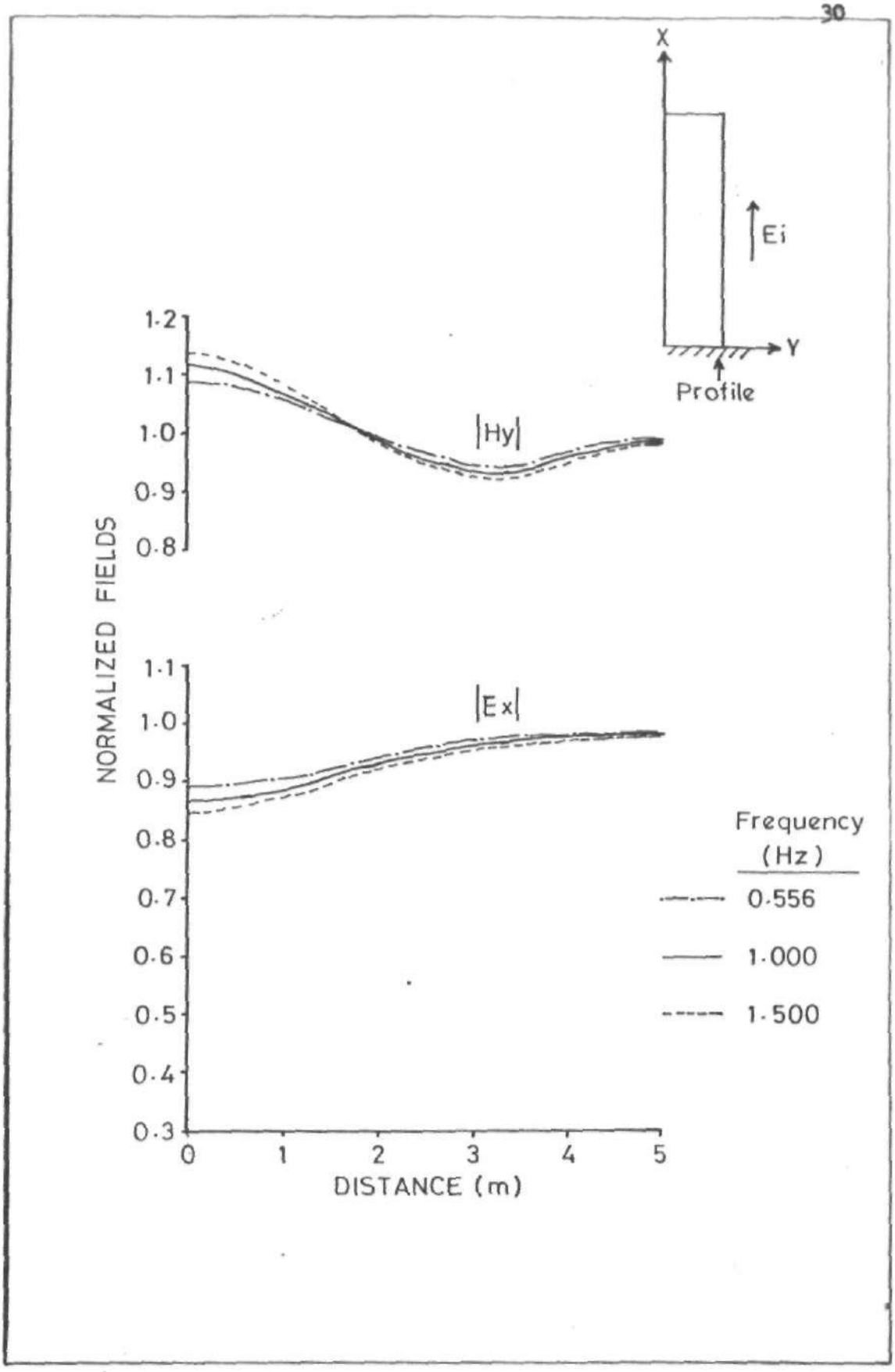


FIG. 4.3 Spatial variation of E-parallel mode horizontal field components of a 3-D body (aspect riotio = 4). Ei is the incident electric field.

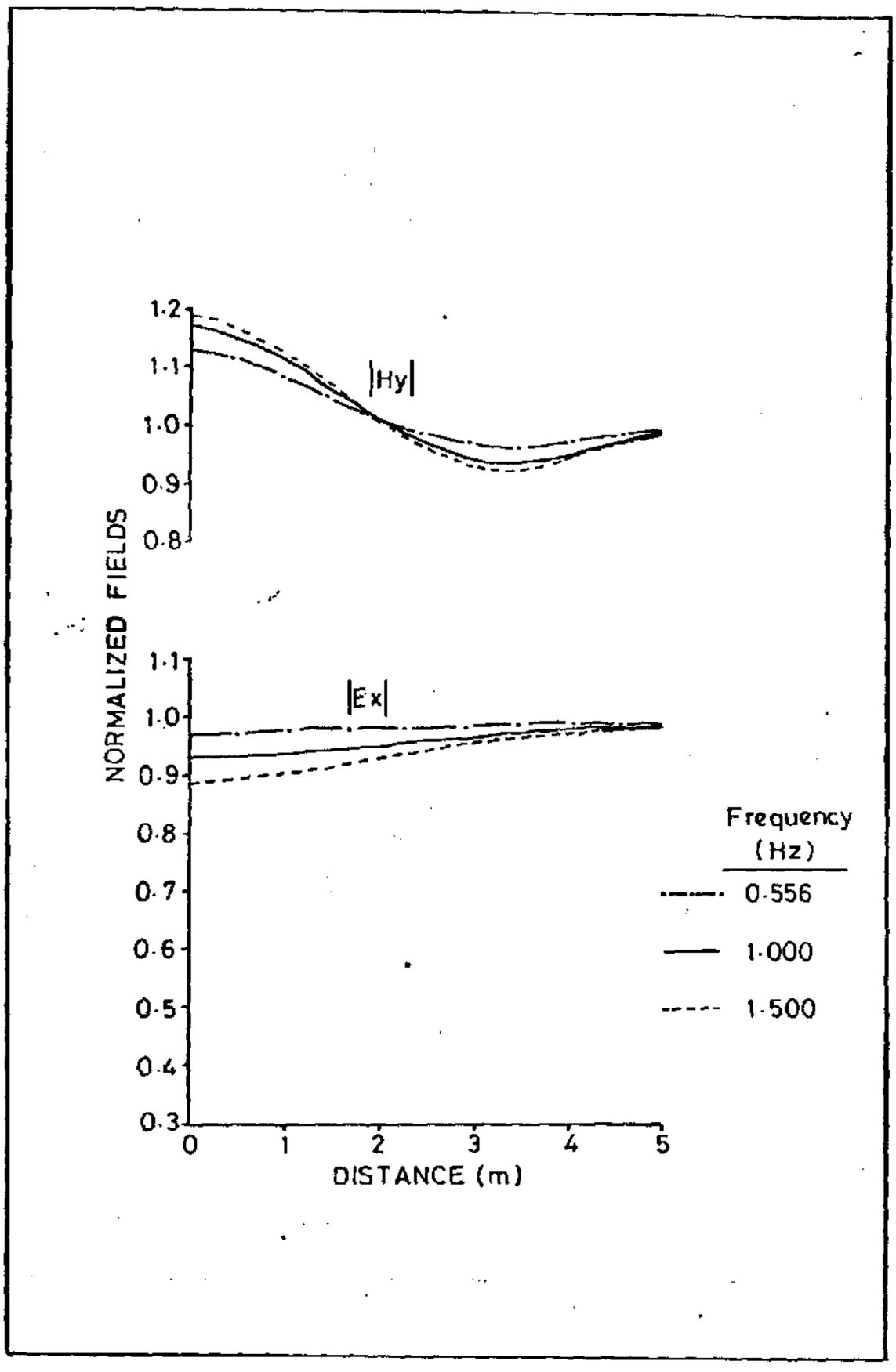


FIG. 4.4 Spatial variation in TE-mode horizontal field components Ex and Hy over a 2-D body.

Only one half of each profile is plotted because of its obvious symmetry.

It is apparent that the effect of the increased aspect ratio of the 3 - D body is to reduce the spatial variation in the electric field component Ex, while increasing that of the magnetic field component, Hy. A comparison of Figure 4.2 with Figure 4.4 shows the fundamental differences in the behaviour or 2 - D and 3 - D earth models. Figure 4.2 shows that the spatial variation in the electric field strongly influence the computed apparent resistivity values (proportional to $(E/H)^2$ while in Figure 4.4 the spatial variation in the magnetic field is more important than the spatial variation in the electric field in the calculation of the apparent resistivities particularly at low frequencies.

2 - D TM and 3 - D E - perpendicular modes results are in close agreement (cf Stodt et al, 1981) and are not plotted.

4.3 Model Results and Analysis

The model results are shown in table 4 . 2 which contains the apparent resistivity values and maximum skew values for different aspect ratios of the model and in Figures 4.6 through 4.11 which show the E - parallel mode normalized apparent resistivity curves caluclated at the centre cross-profile transverse to the model long axis and tipper azimuths for the different aspect ratios. The apprent resistivity values are for a site above the symmetry point of the inhomogeneity while the half-space resistivities were used for normalization. The tipper azimuths are for sites in the fourth quadrant (Figure 4.5)

For all the models studied, as the aspect ratio of the 3 - D body is increased the E - parallel mode apparent resistivities approach the TE mode value for the corresponding 2 - D model while the E - perpendicular mode and the corresponding 2 - D TM mode apparent resistivities are in close agreement (cf Newman et al, 1983). These features are easily seen in table 4.2. The first feature above is also seen in the normalized E - Parallel mode apparent resistivity plots in Figures 4.6 through 4.11.

The maximum skew values for all the models dropped very sharply (about 60 percent) when the aspect ratio of the 3 - D body is changed from 2 to 4 and remained almost constant when the aspect ratio is changed from 4 to 6. These are shown in table 4.2. The percent changes in maximum skew values and E - parallel mode apparent resistivities for changes in aspect ratio in all the models are given in table 4.3. The tipper azimuths of the different models for the different aspect ratios were computed and plotted in figure 4.6 through Figure 4 . 11. In general, the long axis of the 3 - D body

Table 4.2 Apparent resistivities and maximum skew for models 1, 2, 3, 4, 5, and 6

Model	Aspect Ratio	Model Size	E - Parallel mode app. res. (Ω.M)	E-Perpendicular mode app. res. (Ω . M)	Maximum Skew
1	2 : 1	4 KM x 2 KM	17 . 8	13 . 8	.149
	4 : 1	8 KM x 2 MK	32 . 0	15 . 1	.062
	6 : 1	12KM x 2 KM	33 . 0	14 . 9	.063
	∞	∞ x 2 KM	35 . 5	14 . 9	.000
2	2 : 1	4 KM x 2 KM	16 . 8	13 . 5	.143
	4 : 1	8 KM x 2 KM	28 . 9	14 . 7	.060
	6 . 1	12KM x 2 KM	29 . 3	14 . 6	.061
	∞	∞ x 2 KM	30 . 7	14 . 7	.000
3	2 : 1	4 KM x 2 KM	15 . 8	13 . 1	.137
	4 : 1	8 KM x 2 KM	26 . 1	14 . 3	.056
	∞	∞ x 2 KM	26 . 9	14 . 3	.000
4.	2 : 1	6 KM x 3 KM	38 . 4	30 . 2	.143
	4 : 1	12KM x 3 KM	66 . 4	32 . 3	.060
	6 : 1	18KM x 3 KM	69 . 1	32 . 1	.061
	∞	∞ x 3 KM	73 . 1	32 . 1	.000
5	2 : 1	4 KM x 2 KM	32 . 0	24 . 9	.149
	4 : 1	8 KM x 2 KM	57 . 6	27 . 1	.062
	6 : 1	12KM x 2 KM	60 . 1	29 . 9	.063
	∞	∞ x 2 KM	63 . 9	26 . 9	.000
6	2 : 1	4 KM x 2 KM	16 . 0	11 . 6	.227
	4 : 1	8 KM x 2 KM	41 . 3	14 . 6	.097
	6 : 1	12KM x 2 KM	42 . 2	14 . 0	.091
	∞	∞ x 2 KM	47 . 4	14 . 3	.000

Table 4.3 Percent changes in apparent resistivities and maximum skew values for different changes in aspect ratio - Models 1, 2, 3, 4, 5, and 6

Model	Percent Change in E-Parallel mode apparent resistivities at the centre when aspect ratio is changed from ∞ to:			Percent change in maximum skew values when aspect ratio is changed from	
	6	4	2	2 to 4	4 to 6
1	5.9	9.9	49.9	58.4	1.6
2	4.6	5.9	45.3	58.0	1.7
3		3.0	41.3	59.1	
4	5.5	9.2	47.5	58.0	1.7
5	5.9	9.9	49.9	58.4	1.6
6	11.0	12.9	66.2	57.3	6.2

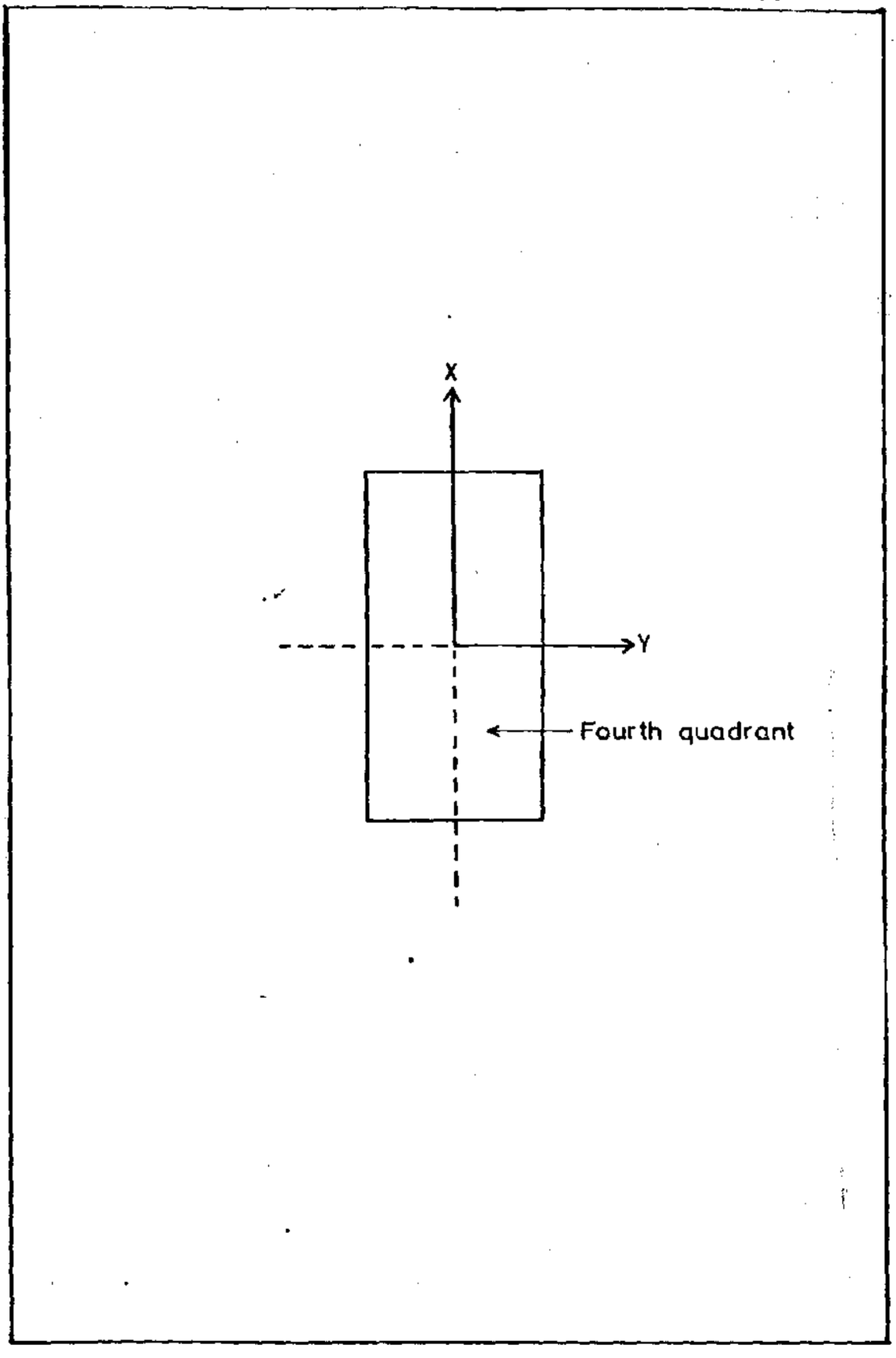


FIG. 4.5 Plan view of a 3-D model.

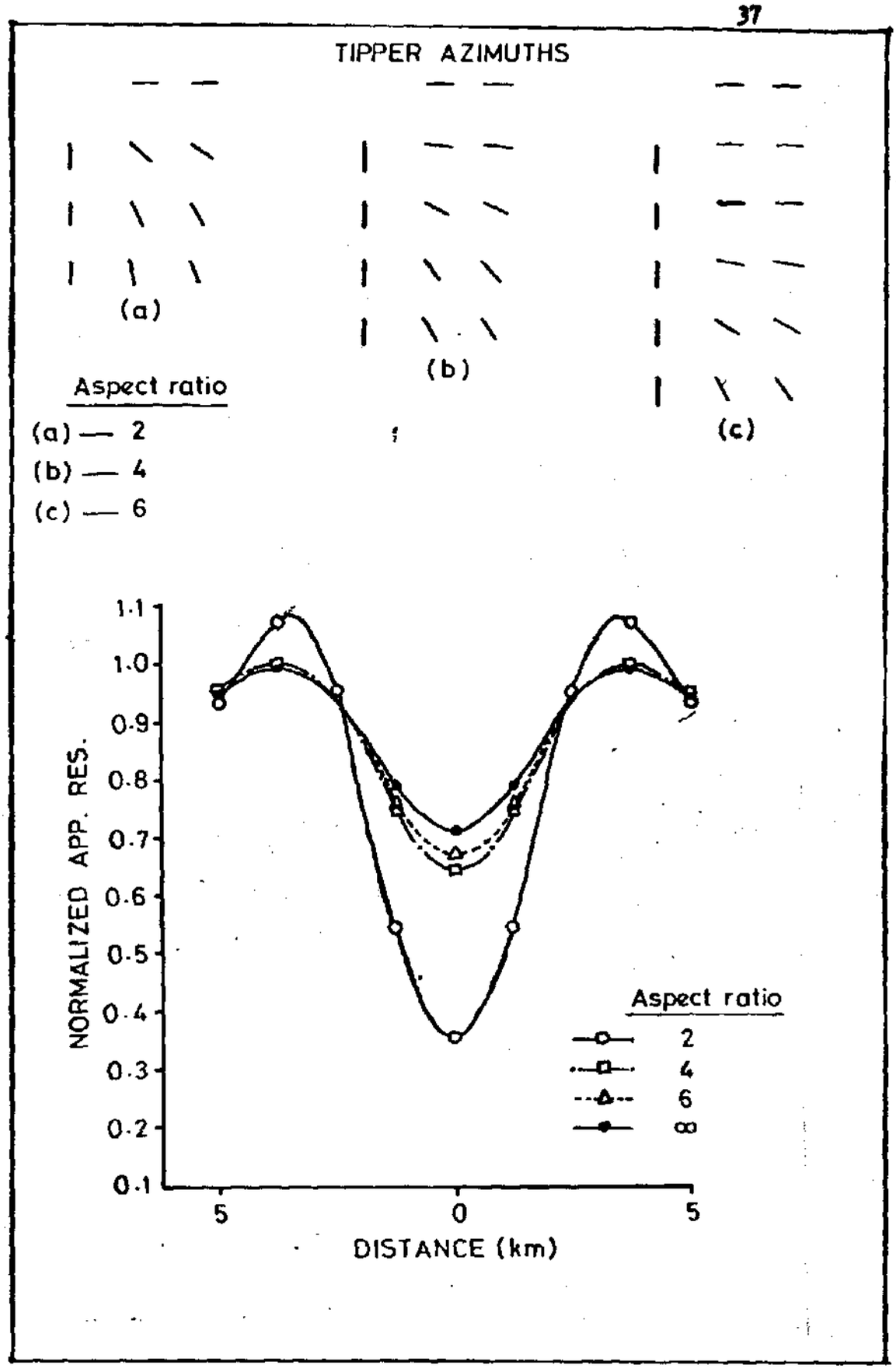


FIG. 4.6 Tipper azimuths and normalized E-parallel mode apparent resistivities – model 1

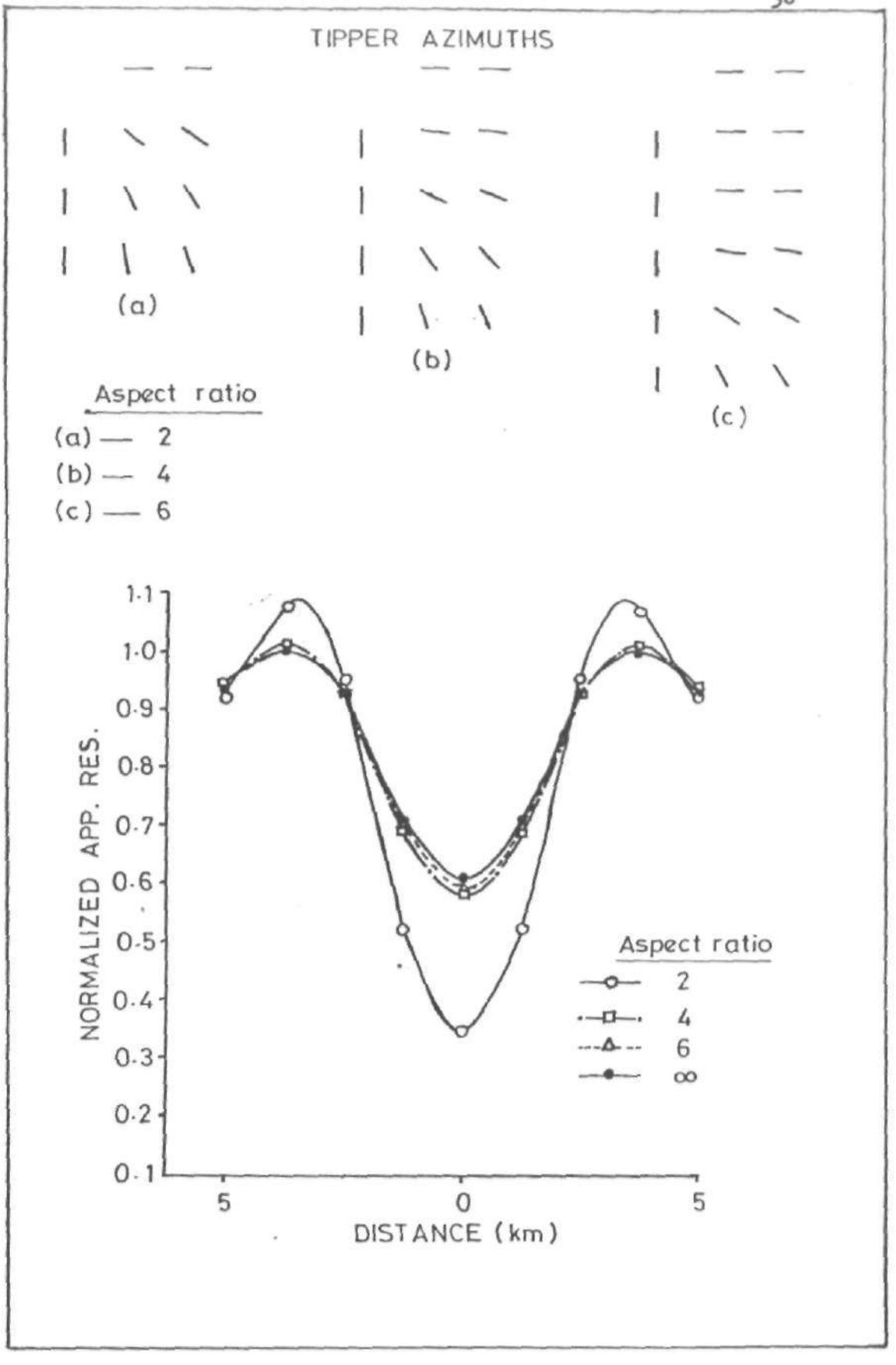


FIG. 4·7 Tipper azimuths and E-parallel mode apparent resistivities - model 2

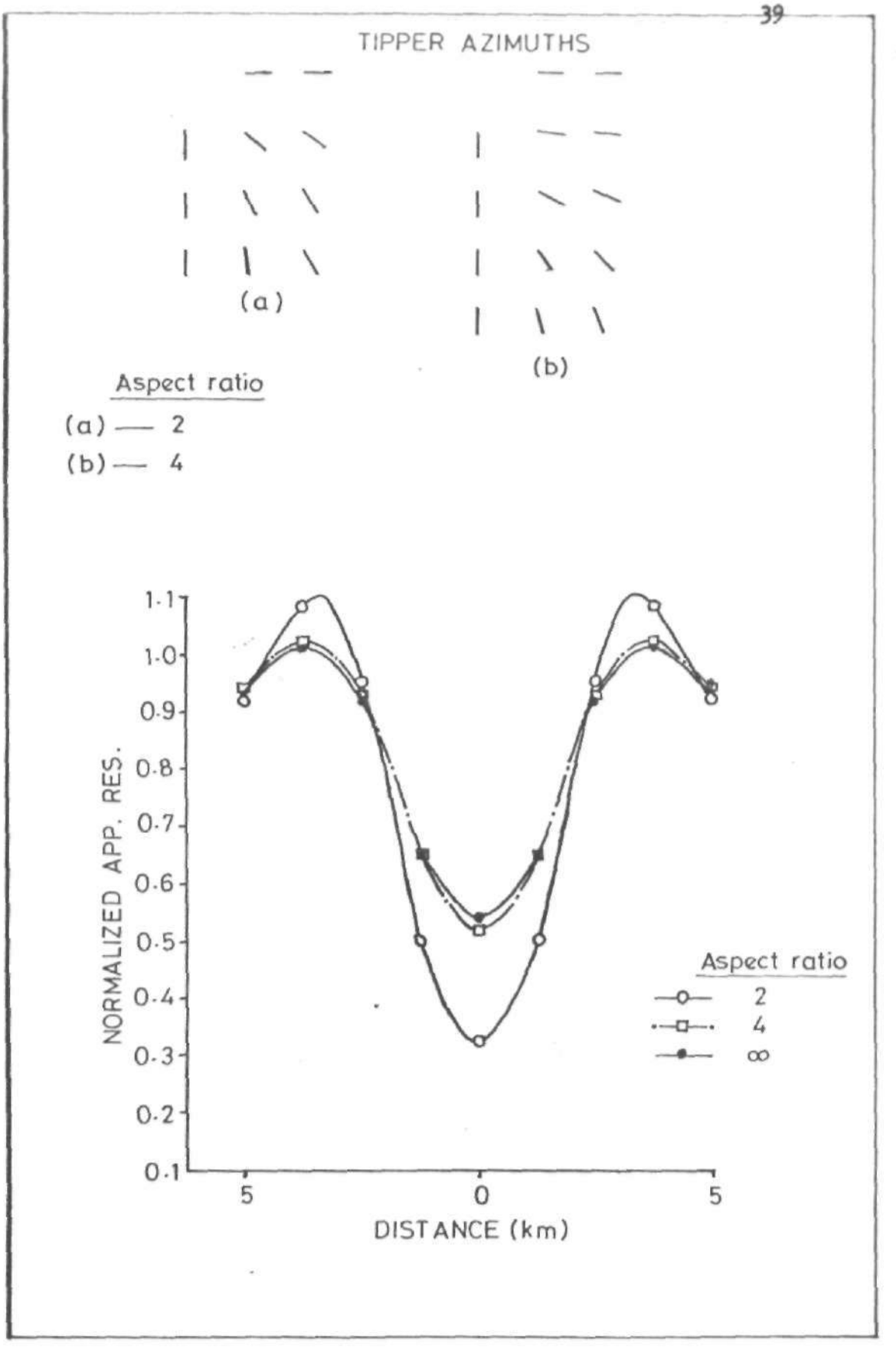


FIG. 4.8 Tipper azimuths and normalized E-parallel mode apparent resistivities - model 3

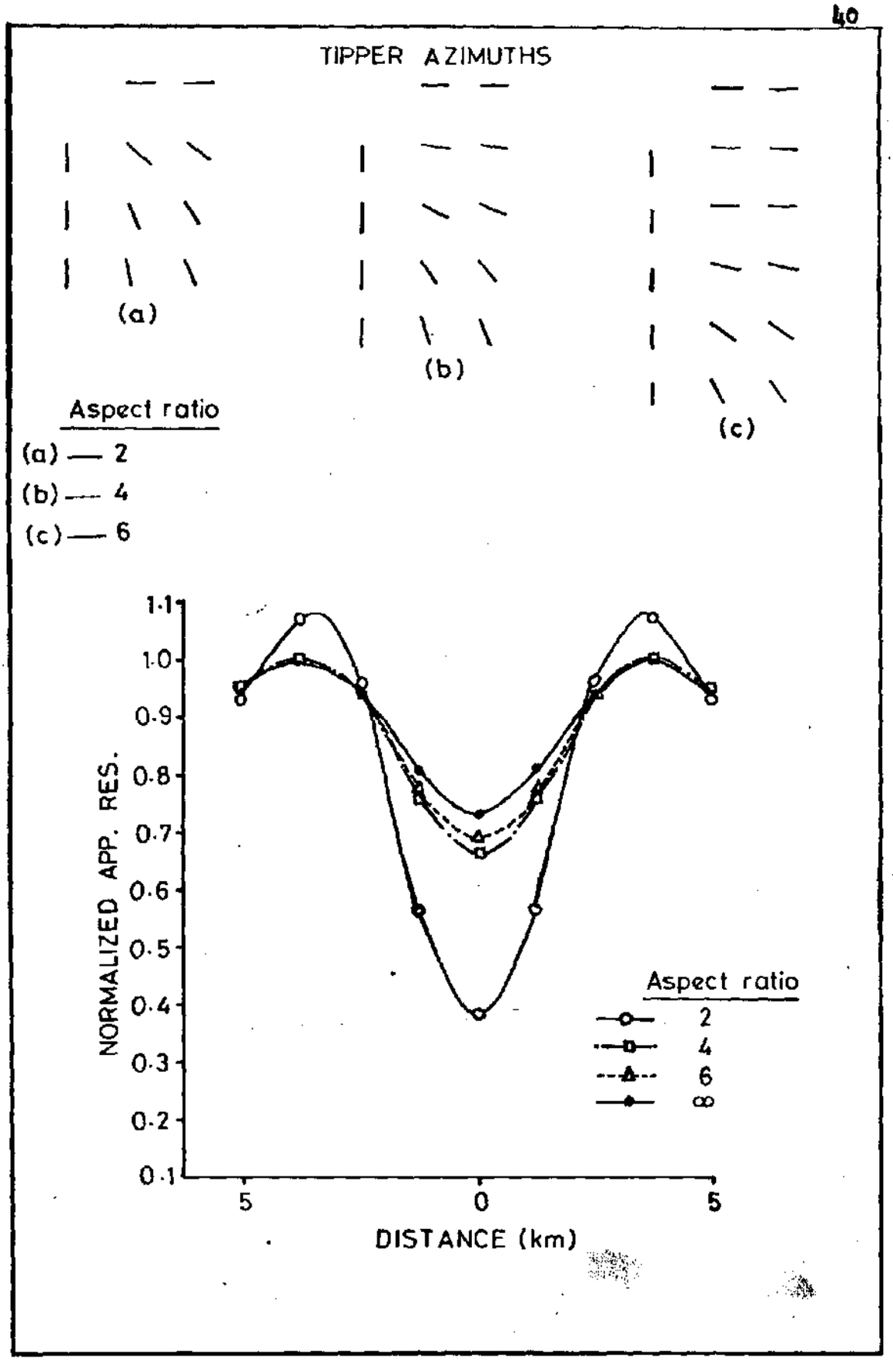


FIG. 4.9 Tipper azimuths and normalized E-parallel mode apparent resistivities - model 4

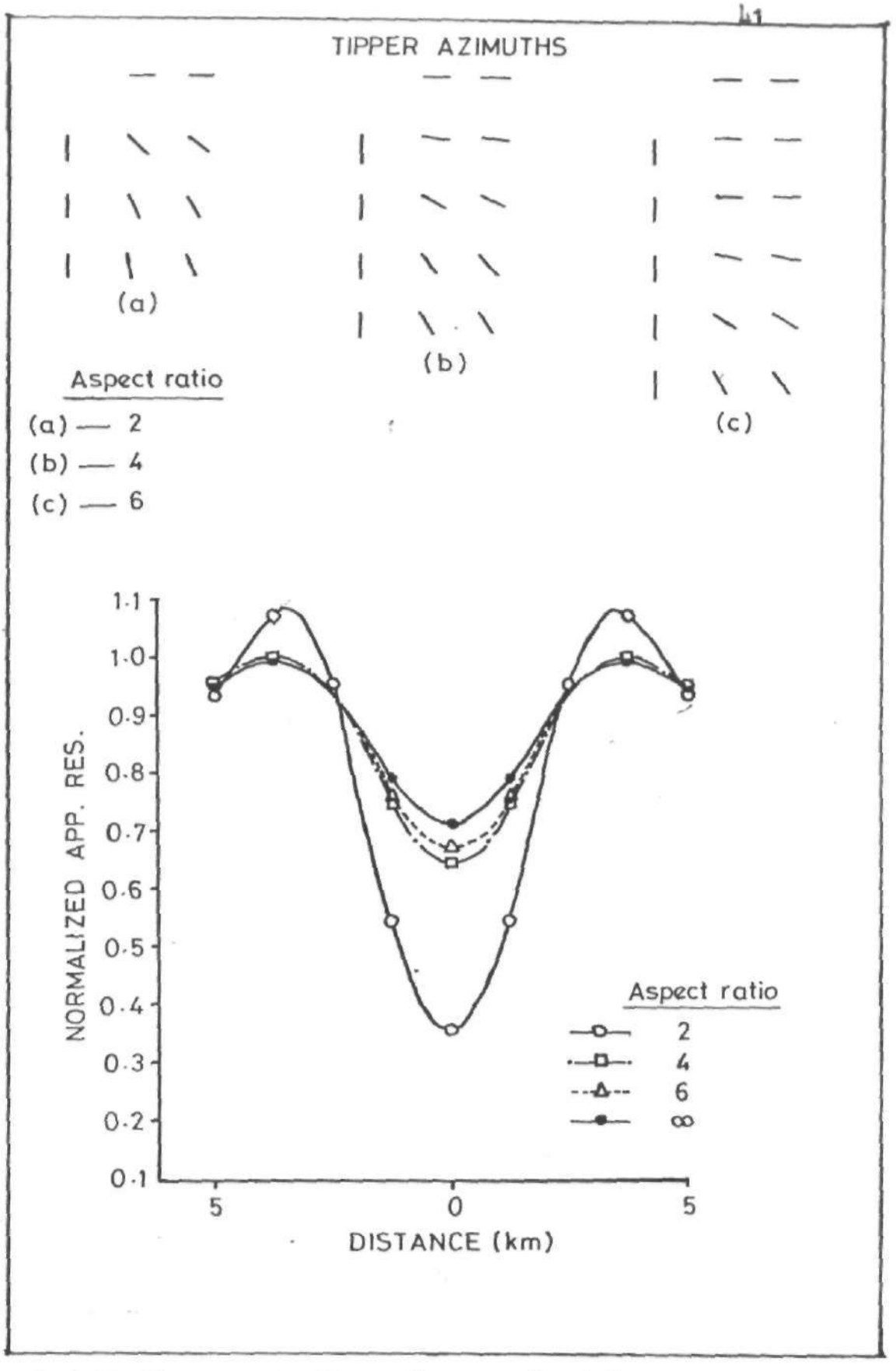


FIG. 4.10 Tipper azimuths and normalized E-parallel mode apparent resistivities – model 5

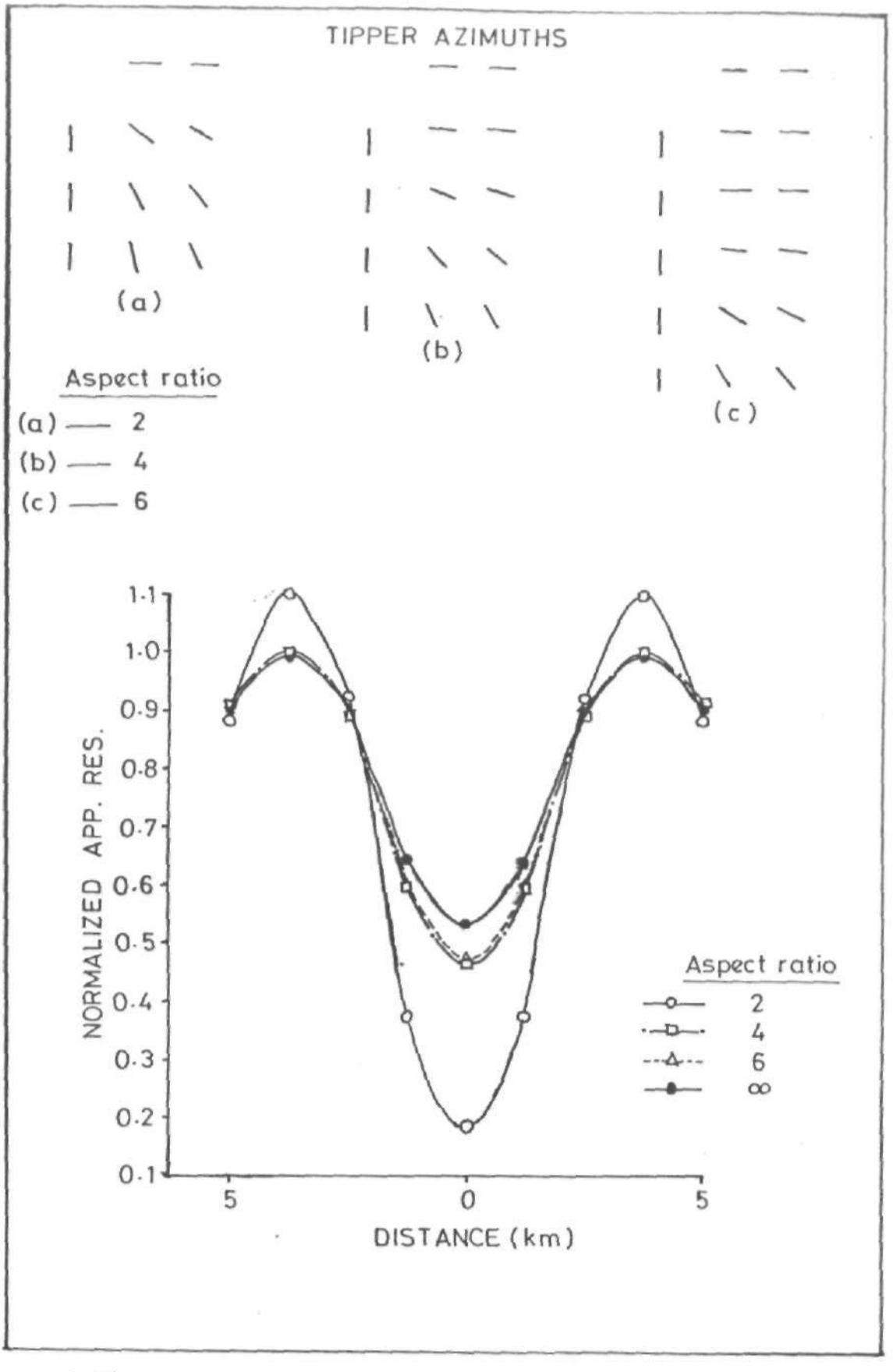


FIG. 4.11 Tipper azimuths and normalized E-parallel mode apparent resistivities — model 6

is indicated by the tipper azimuths around the middle of the inhomogeneities; the degree of indication increasing as the aspect ratio increased (Tippers point 90 degrees to the strike of a 2 - D body as shown in appendix B).

Models 1, 2 and 3 were selected to enable the dependence of the approximation, of a 3 - D body by a 2-D body, on the frequency of the incident waves to be determined. The only parameter which Model 4 has in common with Models 1, 2 and 3 is the resistivity contrast (1 : 10). Models 6 was selected to compare with Model 2 so as to ascertain whether the approximations will be controlled by the resistivity of the half-space while model 5 was selected compare with Model 6; the aim being to determine whether the approximations will be controlled by the resistivity of the inhomogeneity. Model 1 was predicted from Model 5 by invoking electrodynamic similitude discussed earlier. This is clearly shown in table 4.3 where both models have the same percent changes in apparent resistivity and maximun skew values for the same changes in aspect ratio. The scale factor for the apparent resistivities is 1.8, i.e the apparent resistivity values in Model 5 are 1.8 times those in Model 1 (table 4.2).

The tipper azimuths and maximum skew values are the same for both models.

From tables 4.1 and 4.3 it is apparent that as the ratio of the width $2(d1y + d2)$ of the inhomogeneity to the skin depth in the half-space increases the percentage difference between 3 - D E - parallel mode and 2 - D TE mode apparent resistivities decreases. This observation is valid here only for models having resistivity contrast of 1:10 (it will also be valid for contrasts of powers of 1:10 because of electrodynamic similitude). This ratio is a very important quantity in predicting how close to the 2-D TE value the 3-D E-parallel mode result will come at a given aspect ratio. A very simple relationship established for achieving this prediction for two models is given as

$$\left(\frac{\text{Width}}{\delta}\right)_{\text{Model A}} = \left(\frac{\text{Width}}{\delta}\right)_{\text{Model B}}$$

where δ is the skin depth in the half-space. In the above relationship, all the parameters as well as the percentage differences between 2-D and 3-D apparent resistivities for some aspect ratios of one of the models (Model A for instance) are known. When resistivity in Model B is fixed, the relationship yields the frequency of the incident waves for the model. The models in the present study could form a set of different Model A's from which other 3 - D bodies could be approximated with known errors.

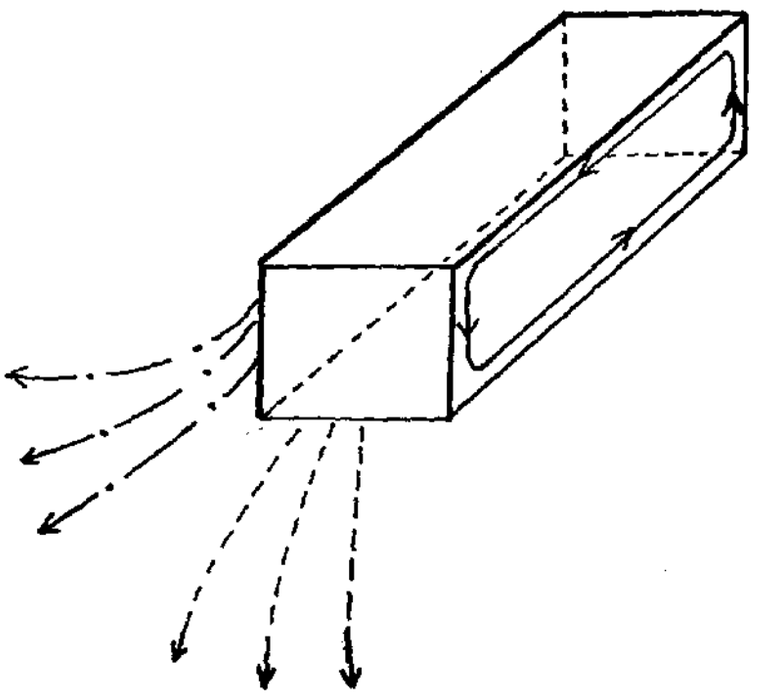
The results obtained for Model 6 shown in table 4.3 are significantly different from those of other models. This is due to the difference in resistivity contrast between model 6 and the

other models. Models 6 has a contrast of 1:18 while the other models have a contrast of 1:10.

The differences and similiarities in the results computed for 2-D and 3-D models can be explained by a study of the electromagnetic field distortions due to these earth models. The distortions of EM fields in conductive 2 - D and 3 - D environments are governed by different mechanisms, namely local induction of current loops and current gathering (vertical and horizontal current gathering), each of which produce different spatial and frequency behaviour in the perturbed fields (Figure 4.12).

In local induction of current loops, the varying regional magnetic field creates local current loops. This local induction is frequency dependent while in current gathering the conductive anomaly can draw currents to itself both vertically and horizontally (vertical and horizontal current gathering respectively). When the thickness of the conductor is small compared to the skin depth in it current gathering has essentially a DC behaviour - their electric field magnitudes are independent of frequency (Park, 1983).

In a 2-D structure where the electric field vector is always aligned parallel to interfaces separating regions of differing conductivity (2-D TE mode) local induction is the only mechanism producing lateral and frequency variation in horizontal EM field components while in the 2-D TM mode, where current flows perpendicular to strike of any conductivity anomaly, the mechanisms are local induction and vertical current gathering. For 3-D structures, all three mechanism contribute to the variations in field components.



Local induction

Horizontal current gathering

Vertical current gathering

FIG. 4.12 Field perturbation mechanisms .

In our 3-D models and for the E - parallel mode, when the aspect ratio is 2 the fields are perturbed mainly by current gathering (vertical and horizontal). This is illustrated in Figure 4.2 where the spatial variations in Ex for all three frequencies are almost the same. The variations in apparent resistivity, proportional to $(E/H)^2$, is a direct result of the electric variation (figure 4.2). The secondary magnetic fields in these cases are only a few percent of the source field. For an induced current flow in the x-direction Ex has low values over the inhomogeneity and the computed apparent resistivities are equally low over the anomaly. In all cases considered the thickness of the anomalous body is small compared to the skin depth in them (Table 4.1).

When the aspect ratio is changed from 2 to 4 (Figure 4.3) local induction becomes more important than current gathering. Induction effects appear as different spatial variations of Ex for different frequencies and general increase in the spatial variation of the magnetic field component, Hy. Current gathering effects are reduced; the decrease can be seen as a progressive decay of the secondary fields, due to interactions with the boundaries, at the measurement sites as aspect ratio is increased (Skin depth rule). The current level is increased but does not equal the ideal 2 - D TE case because current gathering effects are still present. Generally, as induction become more important for increases in aspect ratio, the electric field component, Ex, approaches spatial uniformity while the spatial variation in the magnetic field component, Hy, increases and

the computed apparent resistivities approach their 2 - D TE value. Implicit in the above observations on the spatial variations of Ex and Hy as the aspect ratio is increased, is the fact that the magnetic field around the middle of the inhomogeneity are less affected by the distortions due to the ends of the anomaly as the aspect ratio is increased. The tippers around the middle of the body will thus have azimuths which define the long axis of the inhomogeneity more and more for increases in aspect ratio (i.e. the tippers tend to align themselves perpendicular to the long axis).

The agreement between the 2 - D TM mode and 3 - D E - perpendicular mode apparent resistivities is due to the similarity in the current flow pattern implicit in the formulation of the 2 - D TM problem. Here current flows in vertical planes and perpendicular to the strike of the 2 - D conductive anomaly. Vertical current gathering is the dominant mechanism responsible for the distortion of EM fields in the 3 - D E - perpendicular and 2 - D TM modes; consequently the 3 - D and 2 - D results agree very closely. Increases in aspect ratio in the 3 - D E - perpendicular mode do have some effect but this is very small as horizontal current gathering is of little significance for this mode.

4.4 Applications of the Magnetotelluric Method

The MT method is growing in importance as a geophysical exploration technique. This is due to some advantages the method has over the other major geophysical methods (gravity, seismic, magnetic and d.c. resistivity). These advantages include:

(a) Better estimation of depths; the interpretations of MT data yield true depths and true resistivities, not just anomalies (Vozoff, 1972). Depth interpretation based on MT data is therefore much more definitive than that based on gravity or magnetic data.

(b) Ability to explore seismic blind zones and regions where seismic data are of poor quality, such as those covered by permafrost, volcanics or carbonates.

(c) Easier investigation of deep layers and ability to reach targets seated under resistive screens where d.c. resistivity survey would be difficult to carry out.

(d) Ability to explore formations under highly magnetic layers which would be difficult to detect using the magnetic method.

The method is used in petroleum prospecting in combination with seismic methods and stratigraphic test holes to delineate structures and detect changes in stratigraphy in sedimentary basins (Al'perovich et al, 1977). It has the singular property that it is the only method in oil exploration that can discriminate between superficial and deep conductive layers. It has been extensively applied for regional reconnaissance in the Soviet Union. In such an application, the principal information obtained is the total thickness and conductance of the sedimentary sequence (Al'perovich et al, 1977).

The MT method is also being applied in the exploration for conductive metallic mineral deposits (Strangway et al, 1973, Strangway and Koziar, 1979). Because of the relatively shallow depths and high resistivities encountered in metal exploration, natural fields at high frequencies must be observed. The frequencies used here are in the audio frequency range, and the application has been termed audio-frequency magnetotellurics (AMT).

A third application of the MT method, and one which is growing, is the application to geothermal energy exploration (Wannamaker, 1978; Wannamaker et al, 1979; Park, 1983). Because temperature strongly affects the resistivity of both wet and dry rocks, determinations of Earth resistivity are particularly effective in geothermal exploration (Kaufman and Keller, 1981). The method can be used both in mapping water saturated thermal reservoirs at depths of a few kilometers and in delineating primary heat sources in form of intrusions at depths of 5 or 10 kilometers, or even more.

The approximation of three - dimensional inhomogeneities by two - dimensional inhomogeneities are particularly applicable to conductivity anomalies found in geothermal areas. These anomalies have aspect ratios of up to 5 or more. Wannamaker (1978) and Park (1983) have successfully used 2 - D modeling in place of 3 - D modeling to interprete MT data from the Roosevelt Hot springs geothermal area, Utah, U.S.A. and the Beowawe geothermal area, Neveda, U.S.A. respectively.

CHAPTER V

DISCUSSION AND CONCLUSIONS

The magnetotelluric method in applied geophysics, developed in the 1950's, is a passive technique in which the naturally occuring electromagnetic fields at the earth's surface are used to determine the electrical conductivity distribution within the subsurface. Depending on the nature of the exploration targets one -, two - or three - dimensional earth models are required for quantitative geophysical interpretations.

Maxwell's equations for 1 - D earth can be sovled analytically while for some 2 - D and 3 - D earth models they require the more difficult numerical solutions. However for the 2 - D models, the numerical techniques employed are easy to implement in the computer and pose very little computational problems. For the 3 - D models, the implementation of the various numercial techniques developed (since the mid 1970's) for modeling, have posed severe computational problems. One of these is that they require very large computer storage allocation; another is that excessive computer times are needed. CPU times for 3 - D modeling range from 30 minutes for Daniyan's (1983) Rayleigh - FFT technique for one source polarization to 20 hours for Wannamaker et al (1982) integral equation technique. The CPU times in the present work was about 34 minutes for one source polarization on a cyber 72. These problems have resulted in prohibitive computing costs which together with the very expensive procedure of collecting data from the field in a grid pattern make 3 - D surveys and

interpretations far less attractive than 2 - D ones.

These facts led some researchers notably Weidelt (1975), Ting and Hohmann (1981), Daniyan (1983) and Park (1983) to investigate the circumstances under which a 3 - D body may be approximated by a 2 - D body so that 3 - D surveys and modeling will be carried out only in situations where they are inevitable.

The results presented by the various workers though very enlightening for MT interpretations showed that more work is needed in order to set meaningful guidelines concerning the approximation of 3 - D bodies by 2 - D bodies. We have here, carried further the work started by these workers.

3 - D and 2 - D computer programs developed by Daniyan (1983) and based on the Rayleigh - FFT numerical technique were used for the 3 - D and 2 - D modeling in this study. The technique is valid for curved interfaces separating regions of differing conductivity. Electric and magnetic fields at the earth's surface were computed for some conductive inhomogeneities at different aspect ratios and frequencies. The behaviour of the resultant apparent resistivities, skew and tipper azimuths at the different aspect ratios were investigated. Also investigated is the behaviour of these quantities when electrodynamic similitude is invoked.

The behaviour of the apparent resistivities over a 3 - D (aspect ratio of 2) anomaly is very different in the two cases of E - parallel and E - perpendicular polarizations. In the E - parallel mode the apparent resistivity is significantly

different from the 2 - D TE mode value. This behaviour of the E - parallel mode apparent resistivity is attributed to the different mechanisms which govern the distortion of the electromagnetic fields on and off conductive 2 - D and 3 - D structures. These mechanisms are current gathering (vertical current gathering and horizontal current gathering) and local induction of current loops. Current gathering is the dominant mechanisms responsible for the distortion of electromagnetic fields on and off the conductivity anomalies when aspect ratio is not greater than 2 while local induction of current loops is the only mechanism in the 2 - D TE mode. However as the aspect ratio of the 3 - D body is increased the 3 - D results approach the corresponding 2 - D values; local induction becomes more important than current gathering for increases in aspect ratio and consequently the computed apparent resistivities approach the 2 - D TE value. Also as the frequency of the incident waves is increased the difference between the 3 - D and 2 - D results is reduced. Generally as the ratio of the width of the inhomogeneity to the skin depth in the half-space increases the 3 - D E - parallel mode apparent resistivities move closer to the 2 - D TE value; for instance, for our models with resistivity contrast of 1 : 10 and aspect ratio of 4, when this ratio is 0.419, 0.422, 0.562 and 0.689 the percentage difference between the 2 - D and 3 - D values is 9.9, 9.2, 5.9 and 3.0 respectively. These values can be used in predicting the percentage difference between 2 - D and 3 - D results of a given model. A very simple relationship between two

models, namely

$$\left(\frac{\text{Width}}{\delta}\right)_{\text{model A}} = \left(\frac{\text{Width}}{\delta}\right)_{\text{model B}}$$

is established for selecting the right frequency for this prediction when resistivities are fixed. Here, δ is the skin depth in the half-space. The parameters as well as the percentage differences between 2 - D and 3 - D apparent resistivities of one of the models (Model A for instance) are known; the relationship yields the frequency of the incident waves for Model B. The models in this study could be used as a set of Model A's for approximating other 3 - D models. For the frequencies (0.556 hz, 1.00 hz and 1.50 hz) used here it is found that the aspect ratio of the 3 - D body need not be very large for the apparent resistivities to be within a few percent of the value for the corresponding 2 - D model.

In the E - perpendicular mode, the 3 - D and 2 - D TM mode apparent resistivities agree very closely (cf. Newman et al, 1983). Vertical current gathering is the dominant mechanism responsible for the distortion of EM fields for both modes.

The tipper azimuths around the middle of the inhomogeneities indicated the direction of the long axes of the inhomogeneities with increasing degree as the aspect ratios are increased (Figures 4.6 through 4.11). This is due to the decrease in the perturbation of the magnetic fields around the middle of the inhomogeneities by the ends of the anomalies as the aspect ratios are increased. Consequently the tippers around the middle of the bodies will tend to align themselves perpendicular to the long axes of the bodies.

The maximum skew values dropped sharply (about 60 percent) when the aspect ratio is changed from 2 to 4 and remained constant for a change from 4 to 6 (table 4.2).

When the condition for similitude to exist between two models is satisfied, it is found that the apparent resistivities are appropriately scaled while the skew values, tipper magnitudes and tipper azimuths are the same for both models. The above facts were used to reduce computational effort in this work.

The approximations of 3 - D inhomogeneities by 2 - D inhomogeneities are useful in geothermal areas where conductivity anomalies having aspect ratio of up to 5 or more exist.

Since the numerical technique used here is valid for curved interfaces, it is suggested that studies similar to those in this work be carried out using the other numerical techniques (valid for inhomogeneities with rectangular cross-sections) and comparing the results, though in a gross sense, with those of the present studies. In addition, the studies should be extended to include other magnetolelluric quantities. By so doing, it is anticipated that the result would be a better understanding of the approximation of three - dimensional inhomogeneities by two - dimensional inhomogeneities in magnetotelluric interpretation.

APPENDIX A

SOLUTION TO THE PARTIAL DIFFERENTIAL EQUATIONS

The partial differential equations for 2-D and 3-D models (equations (5), (6) and (7)) are difficult to solve analytically for a general model. However by reducing them to ordinary differential equations the complexity of the problems are greatly reduced. This can be achieved by using the Fourier Integral transform technique which is illustrated here for the 2-D case. The 3-D case is a logical extension of the 2-D solutions and has been treated in detail by Daniyan (1983).

The transform and its inverse are defined by

$$F^{+}(\eta, z) = \int_{-\infty}^{\infty} F(y,z) \exp(-i\eta y)dy \qquad (A\text{-}1)$$

$$F(y, z) = \frac{1}{2\pi} \int_{-\infty}^{\infty} F^{+}(\eta, z) \exp(i\eta y)d\eta \qquad (A\text{-}2)$$

also differentiating equation (A-2) with respect to y yields.

$$\frac{\partial F}{\partial y} = \frac{1}{2\pi} \int_{-\infty}^{\infty} i\eta F^{+}(\eta, z) \exp(i\eta y)\, d\eta \qquad (A\text{-}3)$$

The Two-Dimensional Problem

Transverse Magnetic Mode.

The incident magnetic field has the following form:

$$H^{inc} = \left[\exp(-ikz),\ 0,\ 0\right]$$

It is sufficient for this mode to solve equation (6a) for Hx and derive Ey and Ez from equations (6b) and (6c).

From equations (6a), (6b) and (6c)

$$\frac{\partial^2 Hx}{\partial y^2} + \frac{\partial^2 Hx}{\partial z^2} = \hat{Z}\,\hat{Y}\,Hx \qquad (A\text{-}4)$$

Taking the Fourier transform of equation (A-4) along the y-axis gives

$$\frac{d^2 Hx^+}{dz^2} = (\eta^2 + \hat{Z}\hat{Y})\,Hx^+ \qquad (A\text{-}5)$$

The solution of equation (A-5) is

$$Hx^+ = a \exp(\alpha z) + b \exp(-\alpha z) \qquad (A\text{-}6)$$

where $\alpha = (\eta^2 + \hat{Z}\hat{Y})^{\frac{1}{2}}$

Taking the Inverse Fourier transform of equation (A-6) yields

$$H_x = \frac{1}{2\pi}\int_{-\infty}^{\infty}\left[A(\eta)\exp(\alpha z) + B(\eta)\exp(-\alpha z)\right]x \exp(i\eta y)\,d\eta \qquad (A\text{-}7)$$

Equation (A-7) is valid for any electrically linear, isotropic and homogeneous medium.

The magnetic field components in the different regions (Figure 2.1) are:

$$H_{ox} = \exp(-ikz) + \frac{1}{2\pi}\int_{-\infty}^{\infty}\left[A(\eta)\exp(\alpha_o z)\right]dE \qquad (A\text{-}8a)$$

$$H_{1x} + \frac{1}{2\pi}\int_{-\infty}^{\infty}\left[C(\eta)\exp(\alpha_1 z) + D(\eta)\exp(-\alpha_1 z)\right]dE \qquad (A\text{-}8b)$$

$$H_{2x} = \frac{1}{2\pi}\int_{-\infty}^{\infty}\left[E(\eta)\exp(\alpha_2 z) + F(\eta)\exp(-\alpha_2 z)\right] dE \quad \text{(A-8c)}$$

$$H_{3x} = \frac{1}{2\pi}\int_{-\infty}^{\infty}\left[B(\eta)\exp(-\alpha_3 z)\right] dE \quad \text{(A-8d)}$$

From Ampere's law (equation (2a)) the electric field components in the different regions are (using equations (6b) and (6c).

$$E_{oy} = \frac{-k}{\omega\varepsilon}\exp(-ikz) - \frac{i}{2\pi\omega\varepsilon}\int_{-\infty}^{\infty}\left[A(\eta)\exp(\alpha_o z)\right]\alpha_o dE \quad \text{(A-9a)}$$

$$E_{oz} = -\frac{1}{2\pi\omega\varepsilon}\int_{-\infty}^{\infty}\left[A(\eta)\exp(\alpha_o z)\right]\eta dE \quad \text{(A-9b)}$$

$$E_{1y} = \frac{1}{2\pi\sigma_1}\int_{-\infty}^{\infty}\left[C(\eta)\exp(\alpha_1 z) - D(\eta)\exp(-\alpha_1 z)\right]\alpha_1 dE \quad \text{(A-9c)}$$

$$E_{1z} = \frac{-i}{2\pi\sigma_1}\int_{-\infty}^{\infty}\left[C(\eta)\exp(\alpha_1 z) + D(\eta)\exp(-\alpha_1 z)\right]\eta dE \quad \text{(A-9d)}$$

$$E_{2y} = \frac{1}{2\pi\sigma_2}\int_{-\infty}^{\infty}\left[E(\eta)\exp(\alpha_2 z) - F(\eta)\exp(-\alpha_2 z)\right]\alpha_2 dE \quad \text{(A-9e)}$$

$$E_{2z} = \frac{-i}{2\pi\sigma_2}\int_{-\infty}^{\infty}\left[E(\eta)\exp(\alpha_2 z) + F(\eta)\exp(-\alpha_2 z)\right]\eta dE \quad \text{(A-9f)}$$

$$E_{3y} = \frac{1}{2\pi\sigma_3}\int_{-\infty}^{\infty}\left[B(\eta)\exp(-\alpha_3 z)\right]\alpha_3\, dE \quad \text{(A-9g)}$$

$$E_{3z} = \frac{-i}{2\pi\sigma_3}\int_{-\infty}^{\infty}\left[B(\eta)\exp(-\alpha_3 z)\right]\eta\, dE \quad \text{(A-9h)}$$

where $\alpha_o = (\eta^2 - k^2)^{\frac{1}{2}}$, $\alpha_1 = (\eta^2 + i\beta_1^2)^{\frac{1}{2}}$, $\alpha_2 = (\eta^2 + i\beta_2^2)^{\frac{1}{2}}$ and $\alpha_3 = (\eta^2 + i\beta_3^2)^{\frac{1}{2}}$; $K = \omega^2\mu\varepsilon$; $\beta_1^2 = \omega\mu\sigma_1$, $\beta_2^2 = \omega\mu\sigma_2$ and $\beta_3^2 = \omega\mu\sigma_3$; $dE = \exp(i\eta y)d$; $A(\eta)$, $B(\eta)$, etc. are unknown constants.

The expressions for the electric field components in regions 1 through 3 are obtained with the assumption that $\omega\varepsilon \ll \sigma_i$.

Transverse Electric Mode.

In the TE mode the incident electric field is of the form

$$E^{inc} = \left[\exp(-ikz),\ 0,\ 0\right]$$

and it is sufficient to solve equation (5a) for E_x and derive H_y and H_z from equations (5b) and (5c).

From equations (5a), (5b) and (5c).

$$\frac{\partial^2 E_x}{\partial y^2} + \frac{\partial^2 E_x}{\partial z^2} = \hat{Z}\hat{Y}\ E_x \qquad \text{(A-10)}$$

Taking the Fourier transform of equation (A-10) along the y-axis gives

$$\frac{d^2 E_x^{+}}{dz^2} = (\eta^2 + \hat{Z}\hat{Y})\ E_x^{+} \qquad \text{(A-11)}$$

The solution of equation (A-11) is

$$E_x^{+} = a' \exp(\alpha z) + b' \exp(-\alpha z) \qquad \text{(A-12)}$$

where $\alpha = (\eta^2 + \hat{Z}\hat{Y})^{\frac{1}{2}}$

compare equation (A-12) with equation (A-6). Taking the Inverse Fourier transform of equation (A-12) gives

$$E_x = \frac{1}{2\pi}\int_{-\infty}^{\infty}\left[A'(\eta)\ \exp(\alpha z) + B'(\eta)\ \exp(-\alpha z)\right] x$$
$$\exp(i\eta y)\ d\eta \qquad \text{(A-13)}$$

The electric field components in the different regions are:

$$E_{ox} = \exp(-ikz) + \frac{1}{2\pi}\int_{-\infty}^{\infty}\left[A'(\eta)\exp(\alpha_o z)\right] dE \qquad \text{(A-14a)}$$

$$E_{1x} = \frac{1}{2\pi}\int_{-\infty}^{\infty}\left[C'(\eta)\exp(\alpha_1 z) + D'(\eta)\exp(-\alpha_1 z)\right] dE \qquad \text{(A-14b)}$$

$$E_{2x} = \frac{1}{2\pi}\int_{-\infty}^{\infty}\left[E'(\eta)\exp(\alpha_2 z) + F'(\eta)\exp(-\alpha_2 z)\right] dE \qquad \text{(A-14c)}$$

$$E_{3x} = \frac{1}{2\pi}\int_{-\infty}^{\infty}\left[B'(\eta)\exp(-\alpha_3 z)\right] dE \qquad \text{(A-14d)}$$

From Faraday's law (equation (1a)) the magnetic field components in the different regions are (using equations (5b) and (5c).

$$H_{oy} = \frac{k}{\omega\mu}\exp(-ikz) + \frac{i}{2\pi\omega\mu}\int_{-\infty}^{\infty}\left[A'(\eta)\exp(\alpha_o z)\right]\alpha_o dE \qquad \text{(A-15a)}$$

$$H_{oz} = \frac{1}{2\pi\omega\mu}\int_{-\infty}^{\infty}\left[A'(\eta)\exp(\alpha_o z)\right]\eta dE \qquad \text{(A-15b)}$$

$$H_{1y} = \frac{-i}{2\pi\omega\mu}\int_{-\infty}^{\infty}\left[C'(\eta)\exp(\alpha_1 z) - D'(\eta)\exp(-\alpha_1 z)\right]\alpha_1 dE \qquad \text{(A-15c)}$$

$$H_{1z} = \frac{1}{2\pi\omega\mu}\int_{-\infty}^{\infty}\left[C'(\eta)\exp(\alpha_1 z) + D'(\eta)\exp(-\alpha_1 z)\right]\eta dE \qquad \text{(A-15d)}$$

$$H_{2y} = \frac{-i}{2\pi\omega\mu}\int_{-\infty}^{\infty}\left[E'(\eta)\exp(\alpha_2 z) - F'(\eta)\exp(-\alpha_2 z)\right]\alpha_2 dE) \qquad \text{(A-15e)}$$

$$H_{2z} = \frac{1}{2\pi\omega\mu}\int_{-\infty}^{\infty}\left[E'(\eta)\exp(\alpha_2 z) + F'(\eta)\exp(-\alpha_2 z)\right]\eta dE \qquad \text{(A-15f)}$$

$$H_{3y} = \frac{1}{2\pi\omega\mu}\int_{-\infty}^{\infty}\left[B'(\eta)\exp(-\alpha_3 z)\right]\alpha_3 dE \qquad \text{(A-15g)}$$

$$H_{3z} = \frac{1}{2\pi\omega\mu}\int_{-\infty}^{\infty}\left[B'(\eta)\exp(-\alpha_3 z)\right]\eta dE \qquad \text{(A-15h)}$$

α_o, α_1, α_2, α_3, k and dE are the same as those in the TM mode case.

APPENDIX B

MAGNETOTELLURIC QUANTITIES

The MT interpreter should be able to recognize the dimensionality of a structure from field data particularly when this information is not available from geology or previous geophysical work. Usually the electric and magnetic fields themselves are not interpreted since they depend upon the source fields, over which there is no control. Relationships between these fields yield such quantities as impedance tensor and magnetic transfer functions which contain information about the subsurface structure. The impedance tensor and the magnetic transfer function can be manipulated to yield more recognizable quantities such as apparent resistivity, skew, tipper magnitude and tipper azimuth. These quantities are usually studied since they allow for meaningful physical interpretations.

The definitions and computations of the above quantities as well as their behaviour in 2 - D and 3 - D environments are presented.

Impedance Tensor

At a point on the earth's surface the horizontal magnetic and electric fields, at a particular frequency, are related as follows:

$$Ex = Zxx Hx + Zxy Hy \qquad (B - 1)$$

$$Ey = Zyx Hx + Zyy Hy \qquad (B - 2)$$

Or more compactly

$$\left|E\right| = \left[Z\right]\left[H\right] \qquad \text{(B-3)}$$

where $\left|E\right|$ is the vector $\begin{bmatrix} Ex \\ Ey \end{bmatrix}$, $\left[H\right]$ is the vector $\begin{bmatrix} Hx \\ Hy \end{bmatrix}$ and $\left[Z\right]$ is the matrix $\begin{bmatrix} Zxx & Zxy \\ Zyx & Zyy \end{bmatrix}$ and is called the impedance tensor (Ting and Hohmann, 1981).

In 2 - D structures, when the co-ordinate axes are aligned parallel and perpendicular to strike, Zxx and Zyy must be zero. Zxy and Zyx are nonzero and unequal and can be computed using the relations.

$$Ex = Zxy\ Hy \quad \text{and} \quad Ey = Zyx\ Hx.$$

A 90 degrees rotation of the co-ordinate axes results in the same situation except that the Z values are interchanged.

When neither of the co-ordinate axes is along strike, all four elements of the impedance tensor are nonzero and have different values. In this case as well as in 3 - D environments, the tensor elements are solved for by assuming two independent source field orientations in which the magnetic field of the source is in (1) the x - direction and (2) the y - direction. The frequency domain expressions (B - 1) and (B - 2) can be written as

$$\begin{aligned} Ex^1 &= Zxx\ Hx^1 + Zxy\ Hy^1 \\ Ex^2 &= Zxx\ Hx^2 + Zxy\ Hy^2 \end{aligned} \qquad \text{(B-4)}$$

and

$$\begin{aligned} Ey^1 &= Zyx\ Hx^1 + Zyy\ Hy^1 \\ Ey^2 &= Zyx\ Hx^2 + Zyy\ Hy^2 \end{aligned} \qquad \text{(B-5)}$$

where superscripts 1 and 2 refer to the primary fields Hx and Hy respectively.

Simultaneous solution of equations (B - 4) and (B - 5) gives

$$Zxx = \frac{E_x^1 H_y^2 - E_x^2 H_y^1}{H_x^1 H_y^2 - H_x^2 H_y^1}$$

$$Zyy = \frac{E_y^1 E_x^2 - E_y^2 H_x^1}{H_x^2 H_y^1 - H_x^1 H_y^2} \qquad (B - 6)$$

$$Zxy = \frac{E_x^2 H_x^1 - E_x^1 H_x^2}{H_x^1 H_y^2 - H_x^2 H_y^1}$$

$$Zyx = \frac{E_y^2 H_y^1 - E_y^1 H_y^2}{H_x^2 H_y^1 - H_x^1 H_y^2}$$

According to Vozoff (1972),

$$Zxx = - Zyy \qquad (B - 7)$$

and

$$Zxy - Zyx = \text{constant} \qquad (B - 8)$$

for 2 - D structures, while for 3 - D structures Sims and Bostick (1969) found that

$$Zxx + Zyy = \text{constant} \qquad (B - 9)$$

and

$$Zxy - Zyx = \text{Constant} \qquad (B - 10)$$

Apparent Resistivities

After computing the impedance tensor elements the apparent resistivities, ρ, are obtained from

$$\rho_{ij} = \frac{|Z_{ij}|^2}{w\mu} \qquad (B - 11)$$

where i,j is either x or y.

For 3 - D structures, ρ_{xx} and ρ_{yy} have their maximum diagonally off the corners of the structure (Daniyan, 1983). ρ_{xx} and ρ_{yy} have very small values for 2 - D structures in which neither of

the co-ordinate axes is along strike (Vozoff, 1972). xy and yx which are the normal ones investigated show high values off the edges of a conductive inhomogeneity and low values above it (Daniyan, 1983).

Tipper

A relationship similar to equations (B - 1) and (B - 2) can be written between the vertical magnetic field component Hz and the total horizontal field components Hx and Hy, i.e

$$Hz = AHx + BHy \qquad (B - 12)$$

where A and B are unknown complex coefficients known as magnetic transfer functions. The pair of coefficients are thought of as acting on the horizontal magnetic field and tipping part of it into the vertical and for this reason it is called the tipper (Vozoff, 1972).

For a two-dimensional geometry with y - direction across strike (x - direction is along strike),

$$Hz = B\,Hy \qquad (B\ 13)$$

and B is the tipper (Jupp and Vozoff, 1976). In this case the tipper will have an azimuth in the y - direction, which is the direction of most rapid conductivity variation.

For an arbitrary co-ordinate system (2 - D and 3 - D structures) the pair of coefficients (A,B) are solved by imposing two different source polarizations as in the impedance tensor problems.

The magnitude of the tipper is given as

$$T = \left\{ |A|^2 + |B|^2 \right\}^{\frac{1}{2}} \qquad (B - 14)$$

and its direction which is the angle measuring clockwise from the x - axis is

$$\phi = \frac{(A_r^2 + B_r^2)\ \tan^{-1}\left(B_r/A_r\right) + A_i^2 + B_i^2)\ \tan^{-1}\left(B_i/A_i\right)}{|T|^2} \qquad (B - 15)$$

where subscript r means the real part and i means the imaginary part of a complex number.

Skew

Skew is a three - dimensional parameter defined as

$$S = \frac{|Zxx + Zyy|}{|Zxy - Zyx|} \qquad (B - 16)$$

Skew is non-zero for 3 - D structures. The maximum values are somewhat off the corners of the inhomogeneity (Ting and Hohmann, 1981). Skew is zero for 1 - D and 2 - D structures, and along the lines of symmetry for symmetric 3 - D bodies.

REFERENCES

Aki, K. and Larner, K.L, 1970. Surface motion of a layered medium having an irregular interface due to incident plane SH waves. Journal of Geophysical research, 75; No. 5: 933 - 954.

Al'perovich, I.M., Bubonv, V.P. Varlamov, D.A., Konnov, Yu. F., Konavalov, Yu. F., Koshlakov, G.V., Chernyavaskiy, G.A., Sheinkman, A.L. and Yakovlev, I.A., 1977. Effectiveness of Magnetotelluric Exploration for Studying Regions with Oil and Gas Prospects in the USSR. OTzN-TI, Moscow, 119 pp.

Bard, P. and Bouchon, M., 1980(a). The seismic response of sediment - filled valleys. Part 1. The case incident SH waves. Bull. seism. soc. AM., 70: 1263 - 1286.

————————, 1980(b). The seismic response of sediment-filled valleys. Part 2. The case of incident P and SV waves. Bull. seism. soc. Am., 70: 1921 - 1941.

Cagniard, L., 1953. Basic theory of the magnetotelluric method of geophysical prospecting. Geophysics, 18: No. 3: 605 - 635.

Daniyan, M.A., 1983. Theoretical magnetotelluric response for simple three - dimensional models: Ph.D. Thesis, Southern Methodist University, Dallas, Texas.

d'Erceville, I. and Kunetz, G., 1962. The effect of a fault on the earth's natural electromagnetic field. Geophysics, 27; No.5: 651 - 665.

Hohmann, G.W., 1975. Three - dimensional induced polarization and electromagnetic modeling. Geophysics 40; No. 2: 309 - 324.

Hohmann, G. W. , and Ting, S.C., 1978. Three - dimensional magnetotelluric modeling. ESL Final Rpt. 77 77-15, DOE contract EY - 76 - S - 071601, July, 48 p.

Jiracek, G.R., 1973. Geophysical studies of electromagnetic scattering from rough surfaces and from irregularly layered structures: Ph.D. Thesis, University of California, Berkeley.

Jones, F.W., 1974. The perturbation of geomagnetic fields by two - dimensional and three - dimensional conductivity inhomogeneities. Pageoph, 112: 793 - 800.

———————, and Vozoff, K., 1978. The calculation of magnetotelluric quantities for three - dimensional conductivity inhomogeneities. Geophysics, 43; No. 6: 1167 - 1175.

Jupp. D.L. and Vozoff, K. 1976. Discussion on The magnetotelluric method in the exploration of sedimentary basins by K. Vozoff. Geophysics, 41; NO. 2: 325 - 328.

Kaufman, A.Ä. and Keller G.V., 1981. The Magnetotelluric sounding method. Elsevier Scientific Publishing Company, Amsterdam.

Meyer, W.H., 1976. Computer modelling of electromagnetic prospecting methods: Ph.D. Thesis, University of California, Berkeley.

Neves, A.S., 1957. The magnetotelluric method in two-dimensional structures: Ph.D. Thesis MIT.

Newman, G.A., Hohmann, G.W. and Wannamaker, P.E., 1983. Detection of silicic magmain in a layered earth using the magnetotelluric method: Presented at the 53rd Annual International SEG Meeting, September 11, in Las Vegas.

Park, S.K., 1983. Three - dimensional magnetotelluric modelling and inversion: Ph,D. Thesis, MIT

Rankin, D., 1962. The magnetotelluric effect in a dike. Geophysics, 27; No. 5: 666 - 676.

Reddy, I.K., Rankin, D. and Phillips, R.J. 1977. The dimensional medeling in magnetotelluric and magnetic variational sounding. Geophys. J.R. Astr. Soc., 51: 313 - 325.

Senti, R.J. 1981. Geophysical activity in 1981. Geophysics: The Leading Edge of Exploration, 1: No. 4: 30 - 55.

Silvester, P. and Haslam, C.R.S., 1972. Magnetotelluric modeling by the finite element method. Geophysical prospecting, 20; No.4: 872 - 891.

Srivastava, S.P. 1967. Magnetotelluric two and three layer master curves. Dom. obs., Ottawa, Canada, Pub. 35, No. 7.

Stodt, J.A. Hohmann, G.W. and Ting, S.C., 1981. The telluric magnetotelluric method in two - and three dimensional environments. Geophysics, 46; No. 8: 1137 - 1147.

Strangway, D.W., Swift, C.M., Jr. and Holmer, R.C. 1973. An application of audio frequency magnetotelluric (AMT) to mineral exploration. Geophysics, 38: 1159 - 1175.

———————, and Koziar, A., 1979. Audio frequency magnetotelluric sound - a case history of the Cavendish geophysical test range. Geophysics, 44 : 1429 - 14446.

Stratton, J.A., 1941. Electromagnetic theory. McGraw-Hill Book Company, New York.

Swift, C.M., Jr., 1967. A magnetotelluric investigation of an electrical conductivity anomaly in the Southwestern United States: Ph.D. Thesis, MIT.

Ting, S.C. and Hohmann, G.W., 1981. Intergral equation modeling of three - dimensional magnetotelluric response. Geophysics, 46; No. 2: 182 - 197.

Vozoff, K., 1972. The magnetotelluric method in the exploration of sedimentary basins Geophysics, 37; No. 1: 98 - 141.

Wannamaker, P.E. 1978. Magnetotelluric investigations at the Roosevelt Hot Springs KGRA and Mineral Mountains, Utah: Univ. of Utah, DOE/DGE rep. 78 - 1701.a.6.1.

————————, Hohmann, G.W., Sill W.R. and Ward, S.H. 1979. 2 - D and 3 - D modeling with applications to crustal structure and reservior assessment at the Roosevelt Hot Springs, KGRA, Utah: Presented at the 49th Annual International SEG Meeting, November, 7 in New Orleans.

————————, Ward, S.H. and Hohmann, G.W. 1982. Magnetotelluric response of three - dimensional bodies in layered earth. University of Utah, Department of Geology, DOE - IDI2079 - 87, 83p.

Weidelt, P., 1975. Electromagnetic induction in three - dimensional structures. J. Geophysics, 41: 85 - 109.

Yungul, S.H., 1961. Magnetotelluric sounding three - layer Interpretation curves. Geophysics, 26; No. 4: 465 - 473.